THE UNIVERSITY OF OKLAHOMA

GRADUATE COLLEGE

CALCULATION OF SINGLET EXCITON STATES IN MOLECULAR CRYSTALS OF AROMATIC HYDROCARBONS VIA THE TRANSITION DENSITY INTERACTION OPERATOR

A DISSERTATION

SUBMITTED TO THE GRADUATE FACULTY

in partial fulfillment of the requirements for the

degree of

DOCTOR OF PHILOSOPHY

BY

CARL CLEMENT ZINSSER

Norman, Oklahoma

1973

CALCULATION OF SINGLET EXCITON STATES

IN MOLECULAR CRYSTALS OF AROMATIC HYDROCARBONS

VIA THE TRANSITION DENSITY INTERACTION OPERATOR

APPROVED BY

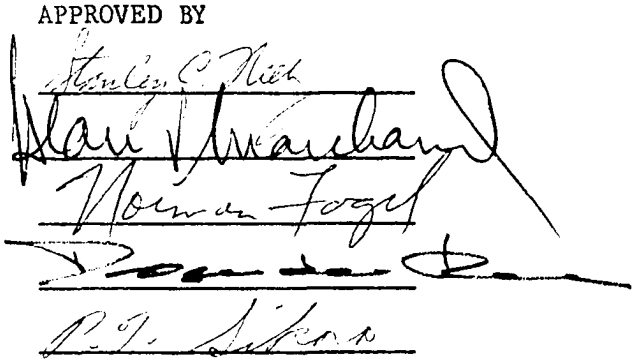

DISSERTATION COMMITTEE

Acknowledgements

I would like to extend my appreciation to Dr. Stanley Neely for suggesting the problem and the members of my committee for their time and consideration. I would especially like to thank Dr. Norman Fogel for his help with space group theory, Dr. Dick van der Helm for aid to my understanding of crystalography and constructive criticisms of this work, and to Dr. Alan P. Marchand for providing me with the opportunity to collaborate on some of his work. I want, also, to thank the Oklahoma University Computer Center for computer time and imparticular Ken Bray for special assistance and Jess May for the use of his program: Thesis Print.

I am deeply grateful for the friendship of Dr. Stanley Neely, whose kindness over the years has not gone unappreciated. Among my other friends who deserve recognition are Dr. Robert Fink, Bill Shepherd, and Chuck Pellerin.

Finally, I want to thank my family for their financial assistance and moral support and especially my wife Judie for her devotion, understanding, and efforts in preparing this manuscript.

TO LUCY

Contents

Tables

Tables cont.

I. Introduction

Since its introduction by Frenkel[1] in 1931, the concept of the exciton has been employed extensively in the study of the optical properties of solids. While considerable effort has been expended in the refinement of the theory and improvements of experimental techniques, one phase of the theory has been consistently neglected, the form of the intermolecular interaction operator.

The optical properties of a molecular crystal differ from those of the isolated constituent molecules principally due to the electrostatic interactions between molecules in the crystal. While the inappropriateness of the point dipole operator to the interactions of extended pi systems has been recognized for some time,[2] with very few exceptions,[2,3,49] it has been applied to these systems.

The principle endeavor reported in this dissertation involves a test of the feasibility of applying the Longuet-Higgins "electric density operator"[4] to the calculation of exciton states in molecular crystals. This operator may be considered as a point-atom approximation as opposed to the dipole operator which is essentially a point-molecule approach. This offers a significant improvement to the calculation of nearest neighbor interactions, which will normally be the predominant terms. In addition there are three characteristics of the interaction included in the electric density operator which are lost in the point dipole approximation: (1) the molecular geometry, (2) the symmetry of the molecular wavefunction, and (3) an implied multipole structure.

The primary system studied in this work is the monoclinic crystal of anthracene. The pioneering application of the electron density operator to exciton calculations was made by Stanley C. Neely,[5] who calculated the coulombic exciton states of BDP (1,5-bis-(Dimethylamino) pentamethinium Perchlorate). Anthracene involves all of the major complications to be encountered in exciton calculations and therefore provides a near ideal system for extending the theory. Also, anthracene is presently the only system for which sufficient effort has been expended in obtaining spectra to allow for a meaningful comparison of theory with experiment. When, however, a comparison is made with another theoretical calculation, tetracene is employed as a second example because its triclinic crystal structure provides a more stringent test of "symmetric" approximations.

Beyond extending the preliminary work on coulombic excitons, the present study provides justification for the mode of calculation and includes the initial application of the operator to the calculation of polaritons.[6]

II. Frenkel Excitons

A. General Description

The term "exciton" was introduced by Frenkel[1] to describe the collective electronic excitations of molecular crystals. In this description the positively charged "hole" left in the ground state configuration and the excited electron form an electrically neutral pair localized on the molecule.

In the first approximation the weak intermolecular interactions leave the manifold of electronic states of each molecule virtually unaltered. If a small but finite crystal field is allowed for, the zero-order functions correspond to non-stationary states in which the probability of finding the excitation on the original molecule decreases with time while the probability density on neighboring molecules increases, spreading the excitation outward through the crystal in a wave-like manner. It was this excitation wave that Frenkel associated with the motion of a quasi-particle, the exciton.

The weak dispersion forces and the small intermolecular overlaps of molecules in molecular crystals allow for a number of simplifying assumptions which make them a preferred testing ground for exciton theories. The basic theory has been discussed in detail in a number of review articles[7,8,9] and monographs[10,11] and will be outlined below to facilitate the interpretation of modifications and extentions introduced by this work and to establish terminology to be used throughout.

The principal approximations assumed to be compatible with molecular crystals are the application of perturbation theory and the construction of Heitler-London wave functions with the omission of antisymmetrization.

The former will be justified later by demonstrating satisfactory agreement with more rigorous approaches,[12,13] while the latter has been vindicated (at least for the systems studied here) by calculations of Rice, et al.[3]

B. One Molecule per unit Cell

The Hamiltonian for a crystal containing N unit cells with one molecule per unit cell is taken to be

$$H = \sum_n H_n + \sum'_{n<m} V_{nm} \tag{2.1}$$

where H_n is the molecular Hamiltonian for the molecule which occupies site n, and V_{nm} the electrostatic interaction operator for molecules at sites n and m. The primed sum indicates the omission of the interaction of molecule n with itself.

If only the first term on the right of (2.1) is retained, the operator corresponds to the "oriented-gas model", and the appropriate wave functions are those of the isolated molecules ϕ_n^f with eigenvalues of energy ε_f for the f^{th} excited state: ϕ_m and ε_0 corresponding to the ground state function and energy respectively. The ground state in this approximation has an energy of $N\varepsilon_0$ and the corresponding Heitler-London wave function is

$$\Phi_G = \prod_n \phi_n^0 . \tag{2.2}$$

The unperturbed excited states corresponding to the excitation of molecule m to its f^{th} excited state will have an energy of $(N-1)\varepsilon_0 + \varepsilon_f$ and a wave function given by

$$\Psi_m^f = \phi_m^f \prod_{n=m} \phi_n^0 . \tag{2.3}$$

Since the excitation can reside with equal probability on any one of the molecules, this represents an N-fold degenerate state and Ψ_m^f is called a

"localized excitation function." The N degenerate functions of type (2.3) may be combined into N orthonormal functions

$$\phi^f(k) = \frac{1}{\sqrt{N}} \sum_n \psi^f_n e^{i\vec{k}\vec{r}_n} \tag{2.4}$$

by the application of space group theory (see section F.) The N "one site excitons" defined in (2.4) are classified by the wave vector $\vec{k}$ given by

$$\vec{k} = \sum_{i=1}^{3} \frac{2\pi K_i}{N_i} \vec{b}_i \tag{2.5}$$

where $\vec{b}_i$ are basis vectors of the reciprocal lattice, and K_i are integers having the values

$$K_i = 0, \pm 1, \pm 2, \ldots + \frac{N_i}{2} \quad i = 1,2,3. \tag{2.6}$$

The vector $\vec{r}_n$ in (2.4) locates m^{th} molecule in the direct lattice with respect to an arbitrary origin.

Reintroduction of the perturbation splits the N degenerate states with functions (2.4) into a band of N quasi-continuous states with energies

$$E_f(k) = \Delta\epsilon_f + D_f + L_f(k) \tag{2.7}$$

where the "exciton coulomb" or "band shift" term D_f is given by

$$D_f = \sum_n' \{(\phi^f_m \phi^0_n | V_{mn} | \phi^f_m \phi^0_n) - (\phi^0_m \phi^0_n | V_{mn} | \phi^0_m \phi^0_n)\} \tag{2.8}$$

and

$$L_f(k) = \sum_m' (\phi^0_m \phi^f_n | V_{mn} | \phi^f_m \phi^0_n) e^{i\vec{k}\vec{r}_m} \tag{2.9}$$

is called an "exciton resonance" or "exciton exchange" term. The band shift term, D_f, is the difference between electrostatic energies of the ground and f^{th} excited state. For molecules without a permanent dipole moment, D_f is incalculable by most approaches and is either omitted or

used as an adjustable parameter. The exciton resonance term (2.9) represents the summed interaction of the transition moment of the n^{th} molecule with all of the other molecules in the crystal. In the initial state $\phi_m^0 \phi_n^f$ the molecule n (at the origin) is in the f^{th} excited state while molecule m is in the ground state. In the final state the opposite is true, amounting to an exchange of excitation.

C. General Exciton Theory: h Molecules per Unit Cell

The equations of the previous section will now be generalized for crystals containing h molecules per unit cell located by the vector

$$\vec{r}_{n\alpha} = \vec{r}_n + \vec{r}_\alpha \tag{2.10}$$

where $\vec{r}_n$ locates the n^{th} unit cell while $\vec{r}_\alpha$ locates the α^{th} site within the cell. The Hamiltonian now involves a sum over Nh molecules

$$H = \sum_{n\alpha} H_{n\alpha} + \sum_{n\alpha \lesssim m\beta} V_{n\alpha,m\beta} \tag{2.11}$$

with the term $V_{n\alpha,n\alpha}$ omitted. The ground state function now has the form

$$\Psi_{n\alpha}^0 = \prod_{n\alpha} \phi_{n\alpha}^0 \tag{2.12}$$

Rather than extend the equation (2.3) in a similar manner, a more convenient choice is to establish a functionllike (2.4) for each site resulting in h "one-site excitons"

$$\phi_{n\alpha}^f(k) = \frac{1}{\sqrt{N}} \sum_n \Psi_{n\alpha}^f e^{i\vec{k}\vec{r}_{n\alpha}} \qquad \alpha = 1,2,\ldots h. \tag{2.13}$$

These one-site excitons can then be combined into h orthonormal functions

$$\Psi_i^f(k) = \frac{1}{\sqrt{h}} \sum_{\alpha=1} B_\alpha^i \phi_{n\alpha}^f(k) \quad i = 1,2,\ldots h \tag{2.14a}$$

or, in terms of the original molecular functions

$$\Psi_i^f(k) = \frac{1}{\sqrt{Nh}} \sum_{\alpha=1}^{h} B_\alpha^i \sum_n e^{i\vec{k}\vec{r}_{n\alpha}} \phi_n^f \prod_{n\neq m} \phi_m^0 . \tag{2.14b}$$

The functions (2.14) are called "factor group functions" or simply "excitons." The coefficients B_α^i can be found by diagonalizing the h X h secular determinant or by utilizing the symmetry properties of the group of the wave vector in which case the subscript i will refer to an irreducible representation of the factor group (section F).

A single non-degenerate molecular state with energy $\Delta\varepsilon_f$ above the ground state will then result in h crystal states of energy

$$\Delta E_f^i = \Delta\varepsilon_f + D_f + L_f^i(k) \qquad i = 1,2, \ldots h \tag{2.15}$$

where the band-shift term is now given by

$$D_f = \sum_m \sum_\alpha \{(\phi_{n\alpha}^f \phi_{n\alpha}^f \,|V_{n\alpha,m\beta}|\, \phi_{m\beta}^0 \phi_{m\beta}^0) - (\phi_{n\alpha}^0 \phi_{n\alpha}^0 |\, V_{n\alpha,m\beta}\, |\phi_{m\beta}^0 \phi_{m\beta}^0)\}\ , \tag{2.16}$$

and the resonance interaction energy is

$$E_f^i(k) = \sum_m{}' \sum_\alpha \{(B_\nu^i)^* B_\mu^i\, e^{ik(r_{n\alpha} - r_{m\beta})} (\phi_{n\alpha}^f \phi_{m\beta}^0 |V_{n\alpha,m\beta}| \phi_{n\alpha}^0 \phi_\beta^f)\}\ . \tag{2.17}$$

D. Correlation with Experiment

The energy difference between the two such exciton states, corresponding to a single molecular transition, is called the "Davydov splitting" and is the principle value used to correlate experiment and theory. Associated with this splitting is the intensity ratio or polarization ratio of the two states. In earlier calculations the theoretical value compared with this observable was the ratio of the crystal transition moments squared. In the calculations reported here the polarization ratio will be taken to be the ratio of oscillator strengths (computed from transition moments and energies obtained after diagonalization of the appropriate

perturbation matrix). These will differ from the former not only in magnitude but, more significantly, in the direction of maximum polarization, thus, providing a third observable to compare with theoretical calculations. At present this is the only theoretical approach predicting this deviation from first order behavior. As a result, experimental investigations have not yet searched for this rotation, although several have alluded to its existence.[14,15]

E. Vibrational Coupling

In the first stage of development of exciton calculations the complexities of a rigorous treatment of the coupling of excitons with both intramolecular and intermolecular vibrations is unwarranted in terms of the limited improvements to calculated observables. The usual treatment is to totally ignore intermolecular vibrations and retain only the intramolecular vibrations which strongly influence the molecular spectra. The coupling cases are distinguished in terms of excitation transger time. An intense transition will normally have a coupling energy much greater than the vibrational energy (c.a. 1500 cm^{-1} for aromatic hydrocarbons) and the excitation will transfer to another site before the molecule can undergo much change of size or shape due to the vibration. This is the "strong coupled"[16] case and is treated as a pure electronic transition. The intermediate case is defined in like manner to involve excitations with transfer times on the order of the vibrational period. Treatment of this case is extremely complicated, and the accepted procedure is to treat it as though the transfer time was long compared to the vibrational period; that is, to treat it as "weak coupled."[16] In the weak coupled case the nuclei can move to a new equilibrium position

before the excitation is transferred and as a result both electronic and vibrational energy are transferred; that is, the transition is vibronic. In accordance with the Born-Oppenheimen approximation the molecular wave function is then given by

$$\phi_{n\alpha}^{f(r)} = \phi_{n\alpha}^{f} \sigma_{n\alpha}^{f(r)} \tag{2.18}$$

where $\phi_{n\alpha}^{f}$ is the pure electronic function and $\sigma_{n\alpha}^{f(r)}$ is a harmonic oscillator wave function in the r^{th} quantum level. The molecular transition moment is now given by

$$M^{f(r)} = (\phi_{n\alpha}^{0} |\vec{\mu}| \phi_{n\alpha}^{f}) \int \sigma_{n\alpha}^{0(0)} \sigma_{n\alpha}^{f(r)} \, d\tau \tag{2.19a}$$

$$M^{f(r)} = M^{f} \xi_{0}^{r} \tag{2.19b}$$

where ξ_0^r is a Franck-Condon overlap factor. The values of ξ_0^r are found from measurements of the intensity distribution in the vapor or solution spectrum, $(\xi_0^r)^2$ being the fraction of the total band intensity found in the r^{th} component, and so

$$\sum_{r} (\xi_0^r)^2 = 1. \tag{2.20}$$

In this approximation each component of the vibronic band is treated as a separate electronic transition with a weighting factor of ξ_0^r. In addition, it is also assumed that the vibrations are totally symmetric and the band is dominated by a single strong progression.

F. Space Group Theory

Since there are a number of detailed discussions of the application of space group theory to excitons available in the literature,[17,18,10] the discussion here will be limited to defining terms and clarifying

the influence of crystal symmetry on exciton states by relying on the formal similarities of space group theory to point group theory and an assumed familiarity with the latter.

The set of translation operators,

$$T_n = n_1 t_1 + n_2 t_2 + n_3 t_3, \tag{2.21}$$

where n_1 are integers and t_1 are primitive translation vectors of the lattice, forms an invariant subgroup of the space group. Since all T_n commute, the subgroup is abelian, and all irreducible representations are one dimensional. To avoid infinite groups, Born von Karmen boundry conditions are imposed so that the lattice repeats itself after N_i (i = 1,2,3) primitive translations and the irreducible representations will be the N^{th} ($N = N_1 \times N_2 \times N_3$) roots of unity,

$$\chi^{(k)}(T_n) = e^{i(k_1 n_1 + k_2 n_2 + k_3 n_3)} \tag{2.22}$$

where

$$k_i = \frac{2\pi K_i}{N_i} \qquad \text{and} \qquad K_i = 0, \pm 1, \pm 2, \ldots, \frac{N_i - 1}{2}. \tag{2.23}$$

The exponent in (2.22) can be expressed as the scalar product of the translation vector and a vector in reciprocal space given by:

$$\vec{k} = \sum_{i=1}^{3} k_i \vec{b}_i, \tag{2.24}$$

where $\vec{b}_i$ is a reciprocal lattice vector defined by

$$\vec{t}_i \cdot \vec{b}_j = \delta_{ij} \text{ and } \vec{b}_i = \frac{\vec{t}_j \times \vec{t}_k}{\vec{t}_1 \vec{t}_2 \times \vec{t}_3} \quad i,j,k, = 1,2,3;2,3,1;3,1,2. \tag{2.25}$$

The parallelepiped enclosing the points defined by the k vectors, as defined in (2.23) and (2.24) is referred to as the main region of nonequivalent (reduced) wave vectors. Alternately, one may choose the region bounded by planes which bisect, and are normal, to the lines connecting the point k = 0 and the nearest points determined by $\vec{g}_m$, where

$$\vec{g}_m = 2\pi \sum_{i=1}^{3} m_i \vec{b}_i \ . \tag{2.26}$$

The latter region is called the first Brillouin zone and contains the whole symmetry of the lattice, each point corresponding to one of the irreducible representations.

For a space group consisting of primitive translations exclusively, the symmetry adapted eigenfunctions belonging to the k^{th} irreducible representation can be obtained by applying the projection operator $O_r^{(k)}$ to the localized excitation function (2.3) to generate the Bloch functions (2.4)

$$O_r^{(k)} \psi_m^f = \frac{1}{N} \Sigma \chi^{(k)}(r_n) \, T_{r_n} \psi_m^f \ , \tag{2.27}$$

where

$$\chi^{(k)}(r_n) = e^{ik \cdot r_n} \quad \text{and} \quad T_r \psi_m^f = \psi_{m+r}^f \tag{2.28}$$

giving, after normalization,

$$\Phi^f(k) = \frac{1}{\sqrt{N}} \sum_n \psi_n^f e^{i\vec{k}\vec{r}_n} \tag{2.4}$$

When dealing with absorption or emission of visible and ultraviolet light, only the representation corresponding to k = 0 needs to be considered. Since k = 0 corresponds to the totally symmetric representation of the translation group, the irreducible representations of the space group coincide with those of the factor group. An element of the factor

group is the product of just one rotation with the entire translation group and, therefore, has the same structure as the underlying point group. These rotations (and reflections) may be combined with fractional translations to form screw axes and glide planes, which transform a member of one sublattice into that of another.

As an example of the creation of factor group functions (2.14), consider the case of anthracene which belongs to the monoclinic system C_{2h}^5. The two molecules contained in a unit cell are related to each other by a two fold screw axis and an ac glide plane, while each site is a center of symmetry. The factor group is, therefore, isomorphic with the point group C_{2h}, while the site group is C_i. (The site group is defined as the group of operations which leave both the molecule and its environment invariant. It is composed of elements which are common to both the factor group and the molecular point group.) In table 1 the characters for the site group C_i are given including the irreducible representations of the molecular point group (D_{2h}) and the factor group (C_{2h}) which correlate with the A_g and A_u representations of C_i.

	(site group)		(molecular point group)	(factor group)
C_i	E	i	D_{2h} correlations	C_{2h} correlations
A_g	1	1	A_g, B_{1g}, B_{2g}, B_{3g}	A_g, B_g
A_u	1	-1	A_u, B_{1u}, B_{2u}, B_{3u}	A_u, B_u

Table 1 The C_i character table with correlations of its irreducible representations to those of both the D_{2h} and the C_{2h} point groups.

A basis function belonging to the irreducible representation B_{1u}, for example, of the free molecule may be reclassified as A_u at a site in the crystal. This in turn correlates with two irreducible representations of the factor group, A_u and B_u, giving rise to two factor group functions from a single molecular state. The factor group functions may be generated by the application of the appropriate projection operator utilizing the characters in table 2.

C_{2h}	E	C_2^b	i	σ^{ac}	
A_g	1	1	1	1	
B_g	1	-1	1	-1	
A_u	1	1	-1	-1	r_b
B_u	1	-1	-1	1	r_a, r_c

Table 2. The C_{2h} character table.

For an A_g site function the indentity and inversion operators transform the first site function into itself while the glide plane and screw axis generate the second site function. When the site representation is A_u, an arbitrary phase must be assigned (as one does with p orbitals) to the result of the last two operations. The usual choice is to define the positive phase to the glide plane as illustrated in (2.29):

$$\begin{aligned} T_{\sigma ac}\Phi_1 &= \Phi_2 & T_E\Phi_1 &= \Phi_1 \\ T_{C_2^b}\Phi_1 &= -\Phi_2 & T_i\Phi_1 &= -\Phi_1 \end{aligned} \qquad (2.29)$$

where the subscript on the wave function refers to the site. Application of the factor group projection operator,

$$O_{\alpha}^{(r)} = \frac{1}{h} \sum_{\alpha} \chi^{(r)}(\alpha) T_{\alpha} \quad , \tag{2.30}$$

where the order of the operation is defined as in, (2,3,1): (2.31)

$$O_{\alpha}^{(r)} = \frac{1}{4} [\chi^{(r)}(E)T_E + \chi^{(r)}(i)T_i + \chi^{(r)}(\sigma^{ac})T_{\sigma ac} + \chi^{(r)}(C_2^b)T_{C_2 b}]$$

produces the following results when operating on an A_u site function (omitting $\frac{1}{h}$):

$$\begin{aligned}
O_{\alpha}^{(A_g)}\Phi_1 &= (1)\Phi_1 + (1)(-\Phi_1) + (1)\Phi_2 + (1)(-\Phi_2) \\
O_{\alpha}^{(B_g)}\Phi_1 &= (1)\Phi_1 + (1)(-\Phi_1) + (-1)\Phi_2 + (-1)(-\Phi_2) \\
O_{\alpha}^{(A_u)}\Phi_1 &= (1)\Phi_1 + (-1)(-\Phi_1) + (1)\Phi_2 + (-1)(-\Phi_2) \\
O_{\alpha}^{(B_u)}\Phi_1 &= (1)\Phi_1 + (-1)(-\Phi_1) + (1)\Phi_2 + (-1)(-\Phi_2).
\end{aligned} \tag{2.32}$$

The first two sums in (2.32) are clearly zero while the latter two give, after normalization,

$$\Psi^{A_u} = \frac{1}{\sqrt{2}} (\Phi_1 - \Phi_2)$$

and (2.33)

$$\Psi^{B_u} = \frac{1}{\sqrt{2}} (\Phi_1 - \Phi_2) .$$

Table 2 indicates that an A_u irreducible representation transforms as a vector on the $\vec{b}$ axis (r_b) while B_u transform as vectors along both the a and c crystal axes. The A_u component will lie in the ac plane. In general, there will be as many components as there are sites in a unit cell, not all of which will correspond to allowed transitions.

G. Selection Rules

Selection rules for the crystal are similar to those for molecular transitions in that the frequency of the radiation (ω) must closely approximate the energy difference between the ground state and an excited state, i.e.,

$$\Delta E = \hbar\omega \ , \tag{2.34}$$

and the crystal transition moment must be nonzero. An additional restriction is imposed by the periodicity of the lattice on the latter condition. If the electric field intensity is given by (2.35):

$$E = E_0 \, e^{-i(\vec{Q}\cdot\vec{r} - \omega t)} \tag{2.35}$$

where E_0 is the amplitude, and Q the wave vector, then the transition probability is proportional to the square of the transition moment M:

$$M = \int \phi_G [eE_0 e^{i\vec{Q}\cdot\vec{r}} r \,] \phi^f(k) \, d_\tau \tag{2.36}$$

or, substituting (2.2) and (2.4) for $_G$ and $^f(k)$:

$$M = \frac{eE_0}{\sqrt{N}} \Sigma e^{i(\vec{k}-\vec{Q})\vec{r}_n} \int \phi_n^0 r \ \phi_n^f \, d_\tau \tag{2.37}$$

The integral in (2.37) is just the transition moment of the molecule at site n, and, of course, must be nonzero. The sum in (2.37) will then be nonzero only if the exponent is zero, that is, if:

$$(\vec{k}-\vec{Q}) \cdot r_n = 0 \tag{2.38}$$

for all values of r_n. This reduces to the condition that k = Q. The wave vector ($Q = \frac{2\pi}{\lambda}$) is very small for ultraviolet and visible light and is taken as zero in the first approximation. This allows the wave functions to be classified in terms of the factor group alone.

III. Lattice Sums in Frenkel Exciton Calculations

A. Dipole-Dipole Sums

The evaluation of matrix elements (2.17) involves a summation of pairwise interactions of a molecule at an arbitrary origin with all other molecules in the crystal. While there appears to be a variety of lattice sum techniques employed in the Frenkel exciton calculations, most can be classified into one of two catagories. The first, the Ewald-Kornfield[19,20] method involves converting an infinite sum over the direct lattice into a double sum over both the direct and reciprocal lattice via a Fourier transform. The advantage of this technique is that the simultaneous sums converge rapidly. The disadvantage is principally the difficulty in applying it. The second classification, which shall be referred to as a Lorentz-Lorenz (LL) sum, involves a direct sum with or without correction terms. The correct application of this approach will be shown to give the same result as the Ewald-Kornfield sum (at least for systems studied here). Incorrect use of direct sums has led to a number of apparently different results for the same calculation and put this approach in a state of illrepute at the present time. Since the calculation of interactions by the electric density model is greatly facilitated by the use of direct sums, the correct procedure will be discussed in detail, but first, the related problem of convergence will be reviewed.

B. Convergence of Dipole Sums

While the convergence of planewise dipole sums is widely recognized, the convergence of spherical sums is still questioned. The usual

argument against convergence involves the fact that the contribution of each interaction is proportional to the inverse cube of the intermolecular separation, R^{-3}, while the number of interactions is proportional to R^3 (i.e., the volume); the implication being that the reduction of each contribution with distance is compensated for by the increasing number of interactions. This line of reasoning ignores the fact that the numerator of the potential (equation 3.5) is proportional to an indirect function of distance:

$$1 - 3\cos^2\theta \tag{3.1}$$

where θ is the angle between the transition moment and the radius vector. Now, although the number of interactions increases with distance, the approximation of replacing $\cos^2\theta$ by its average value simultaneously improves. The average value of $\cos^2\theta$ over a sphere is 1/3,[21] which causes the numerator to approach zero as R increases, and thus, insures convergence.

C. Lorentz-Lorenz Sums

While dipole sums can be expected to converge, the slow rate of convergence generally requires the calculation of long range terms. In Lorenz type calculations the effective field at a point is found by dividing the crystal into a concentric sphere, in which interactions are summed explicitly, and an infinite bulk outside the sphere in which the explicit sum is replaced by an integral over a continuous dipole medium. This configuration is based on the implicit assumption that the effects of anisotropy are short ranged and that ever triclinic systems may be adequately approximated as cubic at sufficiently large separations.

This means that all of the non-cubic character of the sum must be included in the inner sphere and its radius must correspond to the separation at which the cubic approximation becomes valid. Since the value of the inner sphere in the cubic lattice is zero, the sum for non-cubic systems must be carried out until an increase in radius produces a zero contribution to the value of the sum; that is, until convergence. This analysis differs from previous treatments in which the rationalization for summing to convergence was based merely on the grounds of consistency.

The field at site nα due to an oscillating dipole at site mβ may be written as:[22]

$$E_{m\beta} = (\nabla\nabla\cdot - \frac{1}{C^2}\frac{\partial^2}{\partial t^2})\ M_{m\beta} \tag{3.2}$$

where $M_{m\beta}$ is the Hertz vector:

$$M^s_{m\beta} = \frac{M^s_{m\beta}}{R_{m\beta}}\, e^{-i\omega(t-\frac{R_{m\beta}}{C})} \quad . \tag{3.3}$$

In (3.3) $M^s_{m\beta}$ is the transition moment to the s^{th} excited state, $R_{m\beta}$ is the position vector from the origin (nα), and $(t - \frac{R_{m\beta}}{c})$ is the retarded time. The factor $R_{m\beta}/c$ is just the time required for the field to propagate the distance $R_{m\beta}$ at velocity c. With $M^s_{m\beta}$ defined in (3.3), the interaction energy due to the sum of potentials (3.2) for all dipoles in the lattice can be written as:

$$E_{\alpha\beta} = \sum_j{}' e^{i\vec{k}\cdot\vec{R}}\vec{\mu}_i \cdot \{-[\frac{3\hat{R}\hat{R}-1}{R^3}](\cos\vec{kR} + kR\sin\vec{kR}) + k^2\cos\vec{kR} \times [\frac{\hat{R}\hat{R}-1}{R}]\}\cdot\vec{\mu}_j \tag{3.4}$$

where the caps ($\hat{}$) indicate unit vectors and the notation has been abbreviated by using: $i = n\alpha$; $j = m\beta$; and $R = R_{m\beta}$. Now for interactions in the inner sphere, where $kR \ll 1$, (3.4) becomes

$$E \text{ sphere} = - \sum_{j}' \vec{\mu}_i \cdot \left[\frac{3\hat{R}\hat{R} - 1}{R^3} \right] \cdot \vec{\mu}_j \ , \tag{3.5}$$

the familiar static dipole result. For the remaining bulk of the crystal, the summation in (3.4) is replaced by an integral over a dipole continuum with density $\frac{\mu_j}{V}$, V being the volume occupied by the dipole μ_j. The resulting integration from zero to infinity (the lower limit may be either the radius of the sphere or zero since the integral over the sphere vanishes) gives the retarded long range contribution[9]

$$E_{LR}^{Ret.} = \frac{4\Pi}{3V} \vec{\mu}_i \cdot [(3\hat{k}\hat{k} - 1) + \frac{3}{4} (\hat{k}\hat{k} - 1)] \cdot \vec{\mu}_j \ . \tag{3.6}$$

The first term in parenthesis is the contribution from an array of static dipoles, i.e.,

$$E_{LR}^{Stat.} = \frac{4\Pi}{3V} \vec{\mu}_i \cdot (3\hat{k}\hat{k} - 1) \cdot \vec{\mu}_j \ . \tag{3.7}$$

Both (3.6) and (3.7) are nonanalytic functions of k since their limiting value as k approaches zero depends on the direction ($\hat{k}$ being a unit vector in the direction of $\vec{k}$) and not the magnitude. Now unless $\hat{k}$ is perpendicular or parallel to a symmetry element, the scalar product $\vec{k} \cdot \vec{\mu}_\alpha$ will not equal the scalar product $\vec{k} \cdot \vec{\mu}_\beta$ for molecules at sites α and β. In this case, the energy matrix cannot be block diagonalized by symmetry operations of the factor group.

D. Ewald-Kornfield vs. Lorentz-Lorenz Sums

For the purpose of comparison, the explicit sum in the Lorentz-Lorenz (LL) formalism will be abbreviated as Σ_{LL}, and the two terms

in (3.7) as $\hat{k}\hat{k}$ and $\frac{4\Pi}{3V}$ so that the infinite spherical static sum is represented as

$$\Sigma_{LL} + \hat{k}\hat{k} - \frac{4\Pi}{3V} . \tag{3.8}$$

The terms encountered in the Ewald-Kornfield sum are usually abbreviated as

$$t + \hat{k}\hat{k} \tag{3.9}$$

where t is a double sum over the direct and reciprocal lattices and $\hat{k}\hat{k}$ has the same meaning as in (3.8). However, Craig and Walmsley[8] have shown that the spherical depolarization factor of electrostatics may be separated from the double sum and t may be expressed as

$$t = \Sigma_{EK} - \frac{4\Pi}{3V} . \tag{3.10}$$

so that the entire sum becomes

$$\Sigma_{EK} + \hat{k}\hat{k} - \frac{4\Pi}{3V} \tag{3.11}$$

which differs from (3.8) only in the form of the explicit sum. That this was not immediately obvious is due to the way the terms are grouped in the two calculations. In EK sums, the two numerical results obtained are

$$(\Sigma_{EK} - \frac{4\Pi}{3V}) \qquad \text{and} \qquad \hat{k}\hat{k} \tag{3.12}$$

while in the LL sums, they are

$$\Sigma_{LL} \qquad \text{and} \qquad (\hat{k}\hat{k} - \frac{4\Pi}{3V}) . \tag{3.13}$$

In addition, previous applications of LL sums have either omitted the $\hat{k}\hat{k}$ term or both the $\frac{4\Pi}{3V}$ and $\hat{k}\hat{k}$ terms, thus, producing a value for the total sum which bore little or no resemblance to the EK result; had the calculations been made correctly, the results would have been nearly identical, as shown below in Table 3.

Matrix element	Σ_{LL}	$\Sigma_{LL} - \frac{4\Pi}{3V}$	$\Sigma_{LL} + \hat{k}\hat{k} - \frac{4\Pi}{3V}$	$t - \hat{k}\hat{k}$*
Equiv. (1,1)	-.393	-.775	-.660	-.658
Equiv. (1,2)	.370	.370	1.324	1.328
Equiv. (2,2)	2.978	-.609	7.345	7.382
Inequiv. (1,1)	.015	.232	.355	.360
Inequiv. (1,2)	1.393	1.133	2.088	2.088
Inequiv. (2,2)	4.792	1.316	9.278	9.253

Table 3. Matrix elements computed by infinite spherical EK and LL sums for anthracene** (295°K). All energies are in KK (=1000cm^{-1}).
*L.B. Clark and M.R. Philpott, J. Chem. Phys. 53, 3790 (1970)

**Long range terms are for K perpendicular to the (001) crystal plane.

Matrix element	(Site 1)		(Site 2)	
	$\Sigma_{LL} + \hat{k}\hat{k} - \frac{4\Pi}{3V}$	$t + \hat{k}\hat{k}$*	$\Sigma_{LL} + \hat{k}\hat{k} - \frac{4\Pi}{3V}$	$t + \hat{k}\hat{k}$*
Equiv. (1,1)	-.592	-.569	-.745	-.776
Equiv. (1,3)	2.030	1.976	.827	.809
Equiv. (3,3)	9.150	9.157	9.551	9.550
Inequiv. (1,1)	-.174	-.142	-.174	-.142
Inequiv. (1,3)	2.716	2.770	.316	.318
Inequiv. (3,3)	16.303	16.170	16.303	16.170

Table 4. Matrix elements computed by infinite spherical EK and LL sums for tetracene** (295°K). All energies are in KK.
**K perpendicular to the (001) crystal plane.
*L.B. Clark and M.R. Philpott, J. Chem. Phys. 53, 3790 (1970)

Tables 3 and 4 give the results of static sums by the two methods for representive examples: anthracene, which is monoclinic;[23] and tetracene (naphthacene), which is triclinic.[24] Both have two molecules (sites) per unit cell with the first transition along the short molecular axis. It suffices to consider the interactions of just this first transition and the first long axis transition (the second transition in anthracene, the third in tetracene) since in the dipole limit the other elements for a given site can be generated by scaling one of those six. Because the two sites in anthracene are related by a symmetry operation, the sums are independent of the site chosen for the origin. In tetracene, however, where they are not related by a symmetry transformation, a separate calculation is required for each site; producing twelve unique terms. It should be noted that this analysis makes no claim concerning the correctness of either the EK or LL sums but rather is meant to demonstrate the equivalence of the two methods for the systems studied here.

E. Planewise Sums

While the majority of exciton calculations employ spherical sums, a number have been performed in the planewise mode. Proponents of the planewise sums have argued that they are more physically representative since light reflected from a crystal surface is not expected to penetrate to a sufficient depth to justify an infinite spherical environment. Reflection and absorption experiments on a variety of anthracene crystals, however, fail to show a shape

dependence, suggesting that the calculation of interactions should also be shape invariant.

In a recent paper, M. R. Philpott[25] has shown that an infinite planewise sum carried out in what is essentially an Ewald-Kornfield formalism gives the same result as the spherical EK calculation. This prompted the author to attempt the same comparison with direct Lorentz-Lorenz sums. Previously, planewise LL sums have been calculated in a configuration resembling the projection of the unit cell in the plane. In order to facilitate the inclusion of long range terms, which are usually omitted, for the present calculations the plane was divided into two regions: a circle of small radius in which the interactions are summed explicitly; and a dipole continuum for the remainder of the plane. The explicit sum was calculated by using the existing spherical sum program with a simple redefinition of input parameters. The continuum contribution, however, required the derivation (appendix B) of an expression unique to the plane. The form of the long range term in the planewise configuration is

$$E^{\text{Stat.}}_{\text{Plane}} = \frac{\Pi}{A} \vec{\mu}_i \cdot \{(3\hat{k}\hat{k}-1)(\frac{1}{R_0} - \frac{1}{R_f})\} \cdot \vec{\mu}_j \qquad (3.14)$$

where A is the area of the two dimensional unit cell in the plane: μ_i, μ_j the point dipoles; and R_0 and R_f the inner and outer radii respectively. In terms of the spherical correction (3.14) is

$$E^{\text{Stat.}}_{\text{Plane}} = \frac{3}{4} \frac{V}{A} \left(\frac{1}{R_0} - \frac{1}{R_f} \right) E^{\text{Stat.}}_{\text{Sphere}} \qquad (3.15)$$

where V is the volume of the unit cell.

Matrix elements calculated for anthracene in the two geometrical configurations are compared in table 5. In addition to the total sums, the explicit sums excluding long range terms are also reported. The data clearly demonstrates the more rapid convergence of the planewise sums.

Matrix element	$\Sigma^{LL}_{sp.}$	$\Sigma^{LL}_{pl.}$	$\Sigma^{LL}_{sp.} + E_{sp.}$	$\Sigma^{LL}_{pl.} + E_{pl.}$
Equiv. (1,1)	-.393	-.620	-.660	-.657
Equiv. (1,2)	.370	1.206	1.324	1.337
Equiv. (2,2)	2.978	6.618	7.345	7.218
Inequiv. (1,1)	.015	.310	.355	.353
Inequiv. (1,2)	1.393	1.991	2.088	2.086
Inequiv. (2,2)	4.792	8.836	9.278	9.453

Table 5. A comparison of spherical and planewise sums for anthracene. The first two columns compare explicit LL sums for anthracene* in the spherical (sp) and planewise (pl) configurations. The two right hand columns give the same comparison including the long range contributions (sp) and (pl). All energies are in KK.
*K perpendicular to the (001) plane.

An interesting aspect of equation (3.14) is that the value of the long range contribution is a sensitive function of the inner radius (R_0) at which the explicit sum is replaced by an integral over a dipole continuum. The criterion of convergence is not necessary in the plane.

What is required is that R_0 pertain to the distance at which the integrated continuum becomes an adequate approximation of the explicit sum.

The value of R_0 used in all the calculations reported here was 50Å, therefore, the comparison was made for an annular section of the plane with an inner radius R_0 of 40Å and an outer radius R_f of 60Å. Since the dipole continuum is an isotropic approximation, monoclinic anthracene (table 6) and triclinic tetracene (table 7) were again chosen for test cases. The agreement demonstrated in the two tables indicated that a distance of 50Å the continuum approximation is quite good. The adequacy of the approximation has a direct bearing on the accuracy of infinite dipole sums in the LL formalism, for it is this approximation alone which restricts the accuracy.

Matrix element	Σ_{40}^{60}	$\int_{40}^{60}$	$(\Sigma - \int)_{40}^{60}$	$\Sigma_{0}^{50} + \int_{50}^{00}$
Equiv. (1,1)	-.0155	-.0153	-.0002	-.657
Equiv. (1,2)	.0531	.0547	-.0016	1.337
Equiv. (2,2)	.2457	.2503	-.0046	1.328
Inequiv. (1,1)	.0195	.0195	.0000	.353
Inequiv. (1,2)	.0391	.0398	-.0007	2.086
Inequiv. (2,2)	.2543	.2567	-.0024	9.453

Table 6. Explicit sums (Σ) vs. integrals ($\int$) for an annular section of the (001) plane of anthracene (295°K). The first three columns give the energies to the nearest .1cm^{-1} (.0001) kk.

Matrix element	(Site 1) Σ_{40}^{60}	(Site 1) $\int_{40}^{60}$	(Site 2) Σ_{40}^{60}	(Site 2) $\int_{40}^{60}$
Equiv. (1,1)	-.014	-.014	-.020	-.022
Equiv. (1,3)	.072	.071	.018	.019
Equiv. (3,3)	.351	.353	.365	.366
Inequiv. (1,1)	-.013	-.013	-.011	-.013
Inequiv. (1,3)	.065	.069	.017	.020
Inequiv. (3,3)	.355	.360	.346	.360

Table 7. Explicit sums (Σ) compared with integrals ($\int$) for an annular section of the (001) plane of tetracene (295°k). Energies are given to the nearest 1 cm^{-1} (.001 kk).

IV. Exciton Energies

There are presently three principal approaches to the calculation of exciton energies: (1) the perturbation method, (2) the Lorentz oscillator approach, and (3) the second quantized theory. A demonstration of the equivalence of these three methods is desirable not only for the sake of unification but also from the stand point of credibility. For as Hochstrasser noted: "It is hardly encouraging that such a wide variety of theoretical approaches converge on approximately the same result--namely, that obtained from experiment--while at the same time they appear to involve different sets of physical restrictions. One hopes that it may become possible to show the formal relationship between these various methods..."[7] The apparent "wide variety of theoretical approaches" results from combining a variety of lattice sum calculations with a number of different energy calculations. In the preceding chapter the various lattice sum techniques were shown to be equivalent when properly applied. To establish "the formal relationships" then, it only remains to show that the various energy calculations are likewise closely related.

A. Polaritons

The theory outlined in chapter II is essentially a general perturbation approach to Frenkel excitons because the exact nature of the intermolecular coupling was not explicitly stated. It is desirable at this point to redefine the crystal Hamiltonian in a manner which will more clearly establish the nature of the elementary excitations. The Hamiltonian of the crystal and radiation can be

written as[26]

$$H = \sum_i H_i + H_R - \sum_i \mu_i E^{int}(r_i) \qquad (4.1)$$

where H_R is the energy of the transverse radiation field, H_i the adjusted molecular Hamiltonian of the i^{th} molecule in the field of rest, μ_i the transition dipole of the i^{th} molecule located at r_i, and E^{int} the internal electric field at r_i. The entire interaction is now expressed in terms of the internal electric field E^{int}:

$$E^{int} = E^{coul} + E^{tr} \qquad (4.2)$$

where E^{coul} is the coulomb field of the other dipoles and E^{tr} is the transverse field of the radiation. Ball and McLachlan[26] established that the transverse field, E^{tr}, is identical with the transverse part of the classical retarded dipole field. This means that "the internal field in the crystal is the complete retarded field of all molecular dipoles considered as classical radiation sources,"[26] while E^{coul} alone is the corresponding static field.

Two cases are now clearly defined in terms of the interaction field. When the static interaction is employed the energies calculated will correspond to Frenkel's original definition of the exciton. To emphasize the nature of the field this case is sometimes referred to as a coulombic exciton.[27] When comparing these energies with spectra, it is assumed that the radiation must be in resonance with the exciton frequency for absorption to take place. In the second case the retarded interaction couples the exciton to the radiation field and provides a first approximation to a new quasi-particle which is an admixture of an exciton and photon. The coupled particle is referred to as either a polariton[6] or a photoexciton.[11] The resonant frequencies of polaritons

should provide a better estimate of the absorption energies in crystals. It is now possible to establish the equivalence of energy calculations for both excitons and polaritons simultaneously by employing a dipole interaction tensor T_{ij}, in which the field is interpreted as either static for excitons or retarded for polaritons.

B. The Lorentz Oscillator Method

The normal modes of bound particles in the Lorentz model of optical absorption are the classical counterparts of excitons. The quantum mechanical analogue of the classical equations of motion for a set of oscillating dipoles μ_i^n is

$$\left(\frac{\partial^2}{\partial t^2} + \omega^2\right) \mu_i^n = \frac{e^2 f^n}{m} \hat{\mu}_i^n \hat{\mu}_i^n \cdot E_i \qquad (4.3)$$

where n labels the molecular transition, m and e are respectively the mass and the charge of an electron, ω_n and f_n are the isolated molecular transition frequency and oscillator strength respectively, and μ_i^n the unit vector in the direction of the dipole μ_i^n. The exciting electric field at site i, E_i, can be written as the sum of the applied field E_a:

$$E_a = E_0 e^{i(\vec{k} \cdot \vec{r} - \omega t)} , \qquad (4.4)$$

and the dipole exciting field E_d:

$$E_d = - \sum_j{}' \sum_s T_{ij} \mu_j^s , \qquad (4.5)$$

where T_{ij} is the dipole interaction tensor, and $\vec{r}$ is the position vector locating dipole j with respect to dipole i at the origin. The primed sum in (4.5) is over all sites except i, and the unprimed sum over all molecular transitions. If solutions of the plane-wave types are assumed, then

$$\mu_j^n = \mu_{0j}^n e^{i(\vec{k} \cdot \vec{r} - \omega t)} , \qquad (4.6)$$

and equation (4.3) then becomes

$$(\omega_n^2 - \omega^2)\,\mu_i^n = \frac{\hat{\mu}_i^2 e^2 f_n}{m}\left[\mu_i^n \cdot E_a - \sum_j \sum_s \mu_i^n T_{ij} \mu_j^s\right]. \qquad (4.7)$$

This equation, which is also obtained by the second quantized theory,[29] is usually solved in the limit of a very small external field by setting E_a equal to zero. The system of equations is further simplified by approximating μ_i^n in the last term of (4.7) as the transition moment of the isolated molecule. Then, if $\sum_j$, μ_i^n, T_{ij} is abbreviated as T^{ns}, equation (4.7) can be expressed in the linear form

$$(\omega_n^2-\omega^2)\mu^n + \frac{\mu^n e^2 f_n}{m} \sum_s T^{ns} \mu^s = 0 \qquad (4.8)$$

where the subscript i has been dropped. Non-trivial solutions of the linear simultaneous equations (4.8) are found by setting the determinant of the coefficients (of μ^n) equal to zero and solving for the roots.

C. The Perturbation Equations

The equivalence of the second quantized theory with the Lorentz oscillator method has already been established by Craig and Dissado[29] who obtained equation (4.7) from the second quantized equations of energy. To complete the analysis then it is only necessary to show that the perturbation equations can be obtained from (4.7). The first step is to substitute for f_n,

$$f_n = \frac{2m\omega_n d_n^2}{\hbar e^2} \qquad (4.9)$$

in the right hand term where d_n is the magnitude of the n^{th} isolated-molecule transition moment. After multiplying through by $\frac{\hbar}{2\omega_n}$ and making the same approximation which led to (4.8), (4.7) becomes

$$\frac{\hbar(\omega_n^2 - \omega^2)}{2_n} \mu^n + \mu^n \sum_s T^{ns} \mu^s = 0 \quad , \tag{4.10}$$

A trivial solution of (4.10) is $\mu_n = 0$. A non-trivial solution is obtained by solving (4.11).

$$\frac{\hbar(\omega_n^2 - \omega^2)}{2\omega_n} + \sum_s T^{ns} \mu^s = 0 \tag{4.11}$$

The left hand term is simplified by substituting $v = \omega_n - \omega$, so that $\omega^2 = \omega_n^2 - 2\omega_n v + v^2$, and then

$$\frac{\omega_n^2 - \omega^2}{2\omega_n} = \frac{2v\ \omega_n - v^2}{2\omega_n} \tag{4.12}$$

If $\frac{v^2}{2\omega_n}$ is small, which is essentially the applicability requirement for perturbation theory, the left hand term is simplified to $\hbar v$. Now expressing v again as $(\omega_n - \omega)$, equation (4.11) becomes

$$\hbar(\omega_n - \omega) + \sum T^{ns} \mu^s = 0 \tag{4.13}$$

which is the set of simultaneous equations usually encountered in the perturbation approach to exciton energies. When (4.13) is solved by diagonalizing the matrix with elements

$$H_{rs} = \hbar(\omega_n - \omega)\delta_{rs} + T^{ns}\ \mu^{ns} \quad , \tag{4.14}$$

where δ_{ns} is the Kronecker delta, the resultant energies are in good agreement with those obtained from an iterative solution of (4.8). On the other hand, energies calculated by either first of second order perturbation expansions are in poor agreement with either of the former

calculations. This is clearly demonstrated in table 8 which compares the splittings (labeled Sp) and the polarization ratios (PR) for the first three members of the 3800 Å vibronic transition in anthracene.

Trans.		Perturbation (1st order)	Perturbation (2nd order)	Perturbation (Diagonalization)	Iterative solution of Equation (4.8)*
I(0)	Sp:	230	83	260	297
	PR:	(7.5)	(2.6)	(4.0)	(4.9)
I(1)	Sp:	225	-56	106	112
	PR:	(7.5)	(1.4)	(2.5)	(2.8)
I(2)	Sp:	155	-11	55	59
	PR:	(7.5)	(.8)	(2.4)	(2.4)

Table 8. Perturbation calculations vs. an iterative solution. Splittings (Sp) and polarization ratios (PR) for the first three members of the 3800 A transition in anthracene at 295°K and k perpendicular to the (001) crystal plane. Splittings are in cm^{-1} and polarization ratios are dimensionless.
* M.K. Philpott, J. Chem., Phys. 50 , 5117 (1969)

To provide further support for the contention that all dipole calculations are essentially the same when carried out properly, two calculations employing different methods for each step are compared in table 9 for the prominent crystal faces of anthracene. The label "this work" refers to the mode of calculation employing direct (LL) lattice sums and diagonalization of the perturbation matrix. The heading "Philpott" pertains to M.R. Philpott's calculation[14] employing Ewald-Kornfield (EK) lattice sums and an iterative solution of equation (4.8). Both employ the static dipole operator and, therefore, correspond to coulombic excitons. It should be noted that in the paper referred to,[14]

Philpott presents these values as polariton energies. However, the determinental equations used to obtain these energies omit the transverse electric field, a necessary ingredient in polariton calculations. The variation is greatest in the first vibronic member I(0) on each face and decreases with each member of the progression. In particular, the data in the lower left-hand section of table 9 ($\perp$b pol. k$\perp[20\bar{1}]$) suggests that the agreement might be even better if the comparison were more closely controlled in terms of input parameters.

Trans.	p pol. $k \perp (\bar{1}10)$ This work	Philpott	q pol. $k \perp (\bar{1}10)$ This work	Philpott*
I(0)	26.041	26.030	25.640	25.601
I(1)	27.435	27.423	27.148	27.129
I(2)	28.818	28.809	28.644	28.635
I(3)	30.203	30.200	30.132	30.129
I(4)	31.598	31.596	31.560	31.588

Trans.	a pol. $k \perp (001)$ This work	Philpott	b pol. $k \perp (001)$ This work	Philpott*
I(0)	25.688	25.652	25.427	25.355
I(1)	27.170	27.153	27.064	27.041
I(2)	28.648	28.656	28.601	28.589
I(3)	30.137	30.135	30.114	30.110
I(4)	31.564	31.562	31.551	31.547

Trans.	b pol. $k \perp (20\bar{1})$ This work	Philpott	b pol. $k \perp (20\bar{1})$ This work	Philpott*
I(0)	25.918	25.918	25.427	25.355
I(1)	27.326	27.326	27.064	27.041
I(2)	28.750	28.750	28.601	28.589
I(3)	30.179	30.179	30.114	30.110
I(4)	31.588	31.588	31.551	31.547

Table 9. Comparison of two "apparently different" calculations for coulombic exciton states in anthracene (295°K). All energies are in kilokaysers.

*Reference 14.

V. The Transition Density Operator in Exciton Calculations

A. Multipole Calculations

The preceding two chapters serve not only to justify the mode of calculation employed here but also to establish the sameness of calculations within the dipole approximation. Furthermore, the agreement demonstrated in table 9 suggests the futility of attempting to improve the calculations within the dipole framework. This is by no means a general indictment of the dipole interaction operator, but rather, a commentary upon the specific application to extended systems at smaller separations.

The inadequacy of the dipole operator for the systems of interest here has been noted previously[2] and several attempts to include higher multipole terms have been made.[2,3,30] The first of these[2] employed a point-multipole expansion and is subject to the same restrictions as the dipole operator in terms of omitting the molecular geometry and symmetry. The second[3] attempted to evaluate the required integrals employing LCAO wavefunctions of pi electron theory. The principal objection to this method is the heavy reliance on accurate wavefunctions.

The results obtained by either of these methods have been somewhat discouraging, especially in the case of the second transition of anthracene where the predicted splitting is in even worse agreement with experiment than the dipole calculations. Consequently, we seek an alternate means of calculating the short-range interactions.

B. The Electric Density Operator

The intermolecular pair potential for two systems of interacting charges is given by

$$V_{nm} = \sum_{IJ} \frac{Z_I Z_J e^2}{R_{IJ}} - \sum_{IJ} \frac{Z_J e^2}{R_{JI}} - \sum_{Ji} \frac{Z_J e^2}{R_{Ji}} + \sum_{ij} \frac{e^2}{R_{ij}} \quad , \tag{5.1}$$

where Z_I is the atomic number of the I^{th} nucleus and $R_{\alpha\beta} = |r_\alpha - r_\beta|$ (I, J labeling nuclei and i, j labeling electrons in molecules n, m respectively). In terms of the Longuet-Higgins[4] electric density operator, equation (5.1) may be expressed as

$$V_{nm} = \iint \frac{\rho(r_n)\, \rho(r_m)}{|r_n - r_m|} \, dr_n \, dr_m \quad , \tag{5.2}$$

where

$$(r_n) = e \sum_I Z_I \, \delta(r_n - r_I) - e \sum_i \delta(r_n - r_i) \, , \tag{5.3}$$

and $\rho(r_n)$ is defined from (5.3) by replacing the subscripts n, I, i with m, J, j respectively. From the definitive property of the Dirac delta function $\delta(r - r')$:

$$\int f(r')\delta(r - r') \, dr' = f(r) \quad , \tag{5.4}$$

it can be seen that $\rho(r_n)$ is the operator representing the total charge density at r_n; where for example the total electron density at n is given by the expectation value of $e \sum_i \delta(r_n - r_i)$:

$$\int \langle n | \rho(r_n) | n \rangle \, dr_n = \langle n | \int \rho(r_n) dr_n | n \rangle = e\left(\sum_I Z_I - \sum_i 1 \right). \tag{5.5}$$

In (5.5) and what follows $|n\rangle$, $|m\rangle$ are the ground state wavefunctions and $|n'\rangle$, $|m'\rangle$ are excited state functions corresponding to the isolated systems n, m respectively. For a system with zero net charge and no permanent dipole (or multipole) in the ground state, the band shift term (2.16) remains incalculable.

The calculation of splittings and polarization ratios, however, is dependent upon the interactions of transition moments

$$\langle n|M|n'\rangle = \langle n|\int r_n\,\rho(r_n)\,dr_n\,|n'\rangle = \int r_n\,\langle n|\rho(r_n)|\,n'\rangle\,dr_n\,, \tag{5.6}$$

where $\langle n|\rho(r_n)|\,n'\rangle$ is now identified as the charge distribution whose dipole moment is equal to the transition moment between states $|n\rangle$ and $|n'\rangle$. This interpretation allows intermolecular pair interaction to be expressed in a particularly simple form. If we now consider two widely separated systems, such that electron exchange and antisymmetrization can be ignored, the interaction energy is given by:

$$\begin{aligned}\langle nm|V|n'm'\rangle &= \langle nm|\int\int \frac{\rho(r_n)\rho(r_m)}{|r_n - r_m|}\,dr_n dr_m|n'm'\rangle \\ &= \int\int\langle nm|\,\frac{\rho(r_n)\rho(r_m)}{|r_n - r_m|}\,|n'm'\rangle\,dr_n dr_m\,,\end{aligned} \tag{5.7}$$

where the coupled wave function has been taken as a product of the wave functions for the isolated systems. Since $\rho(r_n)$ and $\rho(r_m)$ are associated with the respective systems n and m exclusively, the integration may be carried out over each system separately, and (5.7) becomes

$$\langle nm\,|V\,|n'\,m'\rangle = \int\int \frac{\langle n|\rho(r_n)\,n'\rangle\langle m|\,\rho(r_m)\,|m'\rangle}{|r_n - r_m|}\,dr_n dr_m\,. \tag{5.8}$$

If we now assume that the total charge density associated with an atom can be adequately represented by a single charge, q, situated on the nucleus, (5.8) can be expressed as

$$V_{nm} = \sum_{I,J}\frac{q_I\,q_J}{R_{IJ}}\,. \tag{5.9}$$

This point-atom approximation, while not necessary, does produce a significant reduction in the number of terms. It is conceivable that

an alternate approximation such as locating the charge density at the center of pi orbital lobes might yield better results for the very short separations encountered in dimer and eximer problems. However, a number of variations of this nature applied to the nearest neighbor interaction of crystaline anthracene produced little or no improvement over the point-atom calculation.

C. The Transition Density Multipole Operator

For the purpose of subsequent identification and to emphasize the multipole nature of the interaction, the operator defined by equation (5.9) will henceforth be referred to as the "transition density multipole" operator or simply TDM. This operator will be employed for the short range interactions while the continuous dipole approximation will be used for the long range interactions. The application of this operator to exciton calculations required a knowledge of the atomic coordinates and a set of charge densities. The former is obtained from published crystal structures while the latter can be obtained by scaling transition densities calculated by pi electron theory to give the observed transition moment. The transition densities can be obtained from LCAO-MO theory[41] without explicitly defining the atomic wavefunctions thereby avoiding the strict dependence on good atomic wavefunctions. The resulting charge distribution has the geometry of the molecule and possesses the symmetry of the molecular transition. Preliminary calculations indicate that the nature of the interaction is more dependent upon the molecular geometry and symmetry than the actual charge distribution.

The calculation was first attempted using simple Huckel MO charge densities and later with charges obtained from self consistent field (with configuration interaction) functions.[42] The similarities of these two calculations prompted a series of approximations in which the transitions were represented by various charge configurations. Two of these are included in table 10 along with the MO calculations and the dipole result. The row headed "2 atom" pertains to the calculations in which the transition moment was represented by two charges situated on the appropriate molecular axis with coordinates corresponding to the centers of positive and negative charge of the SCF-CI charge manifolds. This configuration represents a finite dipole. A second approximation labeled "4 atom" involves four charges in a rectangular configuration. This model is more representative of the physical extent of the molecule and possesses the same point group symmetry. The numerical entries in table 10 are the diagonal elements of the inequivalent-site interaction matrix excluding interactions beyond 50 angstroms (the long range contribution being the same additive value for each).

The trends established by employing various charge configurations are well represented by the data in table 10. Any reasonable charge separation produced a negative value for the short molecular axis transitions (I, III, IV), whereas the point dipole produces a positive result. When the distribution reflected the point symmetry and full geometrical extent of the molecule (4 atom, SCF-CI, and HMO) the results were reasonably insensitive to the actual charge distribution.

The results of a previous pi electron method (Rice et. al.[3]) are included for comparison and appear to be more closely related to the dipole results.

	I	II	III	IV
Dipole	.048	4.722	.026	.031
2-atom	-.119	3.488	-.131	-.170
4-atom	-.166	3.942	-.182	-.304
SCF-CI	-.169	3.718	-.181	-.385
HMO	-.181	3.683	-.140	-.434
Rice et. al.*	.016	7.280	**	**

Table 10. Diagonal elements of the interaction matrix via a variety of computational models.
All entries are in kilokaysers
*Ref. 3.
**Values not reported.

D. Application of the Transition Density Operator to Anthracene

Anthracene has become the standard test system for exciton calculations for several reasons. First, its crystal structure is well established,[23] as are the methods of crystal growth and purification. It has three well defined faces (001), ($\bar{1}$10), and (20$\bar{1}$) for which spectra are available at room temperature. (The crystal structure[43] and spectra of the (001) face are also available at liquid nitrogen temperature.) The unit cell contains two inequivalent sites, and therefore, each molecular transition is split into two in the crystal. The isolated molecule has both a very strong (f = 1.6), essentially pure electronic

transition, and a moderately intense (f = .1) vibronic system. Anthracene, therefore, involves most of the complications to be encountered in exciton calculations: but, perhaps, its greatest advantage is that the crystal absorption spectra has received considerably more attention than that of any other molecular crystal.[31-40] However, the techniques are not sufficiently refined to allow an accurate assessment of the splittings and polarization ratios for even this system.

The comparison with experiment is further restricted by theoretical limitations. The inability to calculate the band shift term makes a comparison with the experimental absorption energy meaningless. However, since the band shift term is identical for two factor group components of the same transition, the difference of these two energies (the factor group splitting) can be evaluated theoretically. The corresponding oscillator strengths can also be calculated with some confidence but the measured values in the latter case are a function of the experimental configuration and the true values are difficult to extract. The ratio of two oscillator strengths (the polarization ratio), on the other hand, should be less sensitive to the experimental configuration and therefore provide the most meaningful value to compare with theory. The success of a theoretical approach is accordingly gauged in terms of its ability to reproduce the magnitudes (and trends in the case of a vibronic transition) for the splittings and polarization ratios. A singular exception is the splitting of the first member of a vibronic transition, which is invariably overestimated

by theoretical calculations. This excessive splitting is not yet understood but probably results from approximating the transition as a single vibronic progression.

The appropriate set of splittings and polarization ratios for the three prominent crystal faces of anthracene (at 295°K) are given in table 11.

	(001)		(20$\bar{1}$)		($\bar{1}$10)	
	Sp	PR	Sp	PR	Sp	PR
I(0)	190	4.7	270	16	*	36
I(1)	110	3.2	180	7	110	3.9
I(2)	60	2.8	100	4	90	1,8
II	12,600	.2	2,800	*	600	*

Table 11. Accepted experimental splittings and polarization ratios for anthracene at 295°K.[14]
*Not reported.

The following tables (12-20) contain the results of calculations applicable to the observed values in table 11. With the exception of table 14 (which contains the HMO and "4 atom" results for the (001) face at room temperature) each table reports the results of calculations by the TDM operator (upper half page) and the dipole approximation (lower half page.) The data pertaining to the (001) face is by far the most meaningful since it is representative of estimates extracted from both absorption and reflection spectra, while the values for the remaining faces have been estimated from reflection spectra exclusively.

Comparison of the observed splittings for the first transition of the (001) face (190, 110, 60) with corresponding values in tables 12, 13, 14 shows that reasonable agreement can be claimed for any of the calculations. The closest correspondence, however, is obtained by the retarded TDM (both SCF and HMO) and static dipole calculations. This fact is further emphasized by including the polarization ratios (4.7, 3.2, 2.8) in the comparison. The apparent success of past dipole calculations (for this transition only) can now be seen to be the result of two compensating omissions: (1) the retarded field, which exagerates the splittings (Dipole, table 13) and (2) the inclusion of higher multipoles TDM, table 12), which reduces the splitting.

The latter two refinements fail to cancel in the case of the second transition, where the splitting (12,800) is poorly evaluated by dipole terms alone(either static or retarded) but is in reasonably good agreement with any of the present multipole (TDM) calculations. The same analysis applies to the low temperature calculations for this face (tables 15 and 16). The corresponding splittings (I: 230, 145, 80; II: 13,000) and polarization ratios (I: 5, 4.5, 3.2) both increase with decreasing temperature reflecting the increasing interaction as the lattice contracts.

The calculations pertaining to the $(20\bar{1})$ face (tables 17 and 18) reinforce the trends established in the preceding discussion. The splittings of the first transition (270, 180, 100) are fit equally well by either the retarded TDM (table 18) or static dipole (table 17)

results, while the polarization ratios (16, 7, 4) are in better agreement with the retarded TDM. The splitting of the second transition (2,800) is best fit by the retarded TDM, suggesting once again the previously noted compensation effect. The over all best fit for this face appears to be obtained by the static TDM. This is partially due to the tendency of theoretical calculations to over emphasize the splitting of the first member of a vibronic transition. With this effect taken into consideration, the splittings obtained by the retarded TDM calculation are in better agreement with experiment. The polarization ratios, however, are best fit by the static TDM. This is an isolated departure from the trends established throughout and in the absence of absorption spectra (or at least additional reflection spectra) does not justify speculation as to its cause. The third face ($\bar{1}10$) is probably the most interesting from a theoretical standpoint. The propagation vector for light perpendicular to this face does not lie on a symmetry axis and the usual factor group functions cannot be employed. This means that the full interaction matrix must be diagonalized which results in an unsymmetrical combination of site group functions. Consequently, a molecular transition can split into two crystal transitions which are not necessarily perpendicular as in the previous two cases. Unfortunately, the only spectra available for the ($\bar{1}10$) face[14] were taken in the direction of maximum reflection and perpendicular to it. The maximum reflection occurs in the direction of the intense component of the second transition which lies about four degrees from the

projection of the c axis on this face. Table 21 lists the angles measured from the c axis projection of transition moments corresponding to the four calculations reported in tables 19 and 20. Since the spectra were taken with fixed polarizations and the intensities measured correspond to projections of the transition moments on these directions, the data in these tables cannot be compared directly with experiment. In particular, the splittings may have been measured between false maxima resulting from overlapping projections of close lying transitions. The data in the latter three tables (19-21) can be used to calculate corrected oscillator strengths and polarization ratios. The dipole calculations (Static: 5.5, 3.2, 2.4; Retarded: 2.8, 1.3, .64) show no improvement over the uncorrected values. Including multipole terms by the TDM operator shows no improvement for the static field (2.6, 3.1, 2.4), but a significant improvement results from including both the multipole interaction and the retarded field (TDM Retarded: 24, 3.4, 1.0). In addition, the latter method also gives the best value for the angle of the intense component of the second transition (θ_a, table 21) which is reported[14] to be about 4°.

The analysis of the $(\bar{1}10)$ face indicates the possibility of including the direction of maximum intensity as a third observable to be used in testing exciton calculations. The analysis of all three faces indicates that the apparent success of the calculation for the short axis transition is due to compensating omissions. Furthermore, omitting the retarded field contributions does not compensate for omitting the multipole terms in the case of the long

axis transition. In particular, the reduction of the splitting from the dipole value is due principally to the inclusion of multipole terms by the TDM method.

E. Conclusion

Preciously it was thought that spherical dipole sums were only conditionally convergent and that a technique such as the Ewald-Kornfield or planewise sums was necessary to insure convergence. Furthermore, the Lorentz-Lorenz summation technique had fallen into disrepute because the results failed to agree with those of the accepted methods. During the course of this study it has been established that: (1) the condition for convergence of spherical sums is that the approximation of replacing $\cos^2(kR)$ by its average value improves with increasing radius of interaction; (2) when properly applied the LL technique gives essentially the same results as the EK technique (when $k = 0$); (3) in close agreement with the EK results, the LL sums of the spherical calculations are nearly identical to those of the planewise calculations; and (4) the error introduced by replacing the explicit sum with a continuous dipole is negligible for distances at which it is usually initiated in the LL formalism.

Prior to this study, it appeared that a wide variety of dipole calculations converged on approximately the same result and that perturbation calculations yielded the poorest results. Attempts to include multipole terms gave essentially the same result while inclusion of retardation was strictly detrimental. In this dissertation

it has been shown that the apparent wide variety of energy calculations results from different approximations to the solution of the same series of simultaneous equations. Also, the perturbation approach is as good as any when solved by matrix diagonalization rather than be the first or second order expansions. It has been further noted that previous multipole calculations involved a point molecule approximation which produced results more closely related to the point dipole results than the present multipole calculation reinforcing the observation that the value of the multipole contribution is more sensitive to the molecular symmetry and geometry than to actual atomic wavefunctions or charge distributions employed.

The primary objective of this research has been the application of the transition density multipole operator to singlet exciton states of anthracene. A comparison of this method with the point dipole calculation for the first transition shows that reasonable agreement can be obtained for either method. However, a similar comparison for the second transition demonstrates clearly the superiority of the TDM calculation.

TDM (static) 295°K(001)

Trans.	E_a	E_b	Sp	F_a	F_b	PR
I(0)	25,740	25,669	71	.011	.047	4.2
I(1)	27,201	27,166	34	.007	.024	3.5
I(2)	28,675	28,658	17	.004	.014	3.4
I(3)	30,146	30,140	6	.002	.006	3.3
I(4)	31,569	31,566	3	.001	.003	3.1
II	51,009	37,009	14,000	.309	.032	.1
III	44,578	44,475	104	.076	.173	2.3
IV	56,371	53,031	3,340	.133	.261	2.0

Dipole (static) 295°K(001)

Trans.	E_a	E_b	Sp	F_a	F_b	PR
I(0)	25,707	25,413	294	.014	.062	4.3
I(1)	27,179	27,059	120	.008	.022	2.5
I(2)	28,661	28,599	62	.005	.012	2.3
I(3)	30,139	30,113	26	.002	.006	2.3
I(4)	31,565	31,550	15	.002	.003	2.2
II	59,904	37,027	22,877	.193	.013	.07
III	43,516	44,050	-535	.133	.208	1.6
IV	50,880	52,475	-1,595	.182	.224	1.2

Table 12. TDM vs. Dipole calculations for the (001) face of anthracene at 295°K (static field). Splittings (Sp) are defined as the difference between a- and b-polarized absorption energies: $E_a - E_b$. Polarization ratios (PR) are defined by the ratio of oscillator strengths: f_b/f_a. The data pertains to the first four electronic transitions (I - IV) with the first of these taken as a five member vibronic transition and labeled: I(n), n = 0,...,4. Energies are in cm^{-1}. Oscillator strengths and polarization ratios.

TDM (retarded) 295°K(001)

Trans.	E_a	E_b	Sp	f_a	f_b	PR
I(0)	25,673	25,356	316	.013	.066	4.9
I(1)	27,163	27,044	119	.007	.021	2.9
I(2)	28,653	28,592	61	.004	.012	2.7
I(3)	30,137	30,122	25	.002	.006	2.7
I(4)	31,564	31,550	14	.001	.003	2.7
II	50,147	36,877	13,270	.302	.036	.12
III	44,295	43,907	388	.103	.179	1.7
IV	56,091	52,395	3,697	.092	.213	2.3

Dipole (retarded)

Trans.	E_a	E_b	Sp	f_a	f_b	PR
I(0)	25,619	25,012	607	.017	.081	4.6
I(1)	27,133	26,956	177	.009	.017	1.9
I(2)	28,635	28,010	91	.005	.010	1.9
I(3)	30,128	30,088	39	.003	.005	1.9
I(4)	31,558	31,535	23	.002	.003	1.9
II	59,486	36,974	22,513	.160	.015	.094
III	43,042	43,364	-322	.156	.214	1.4
IV	50,383	51,930	-1,547	.171	.178	1.0

Table 13. TDM vs. Dipole calculations for the (001) face of anthracene at 295°K (retarded field). All energies are in cm^{-1}. Oscillator strengths and polarization ratios are unitless.

TDM (HMO) $295^{\circ}K(001)$

Trans.	E_a	E_b	Sp	f_a	f_b	PR
I(0)	25,684	25,367	316	.013	.067	5.0
I(1)	27,170	27,047	122	.008	.022	2.9
I(2)	28,657	28,594	64	.005	.013	2.8
I(3)	30,139	30,112	26	.002	.006	2.8
I(4)	31,565	31,550	15	.001	.004	2.8
II	50,440	36,891	13,549	.286	.029	.1
III	44,217	43,929	288	.118	.186	1.6
IV	55,880	52,460	3,420	.089	.210	2.4

TDM (4-atom)

Trans.	E_a	E_b	Sp	f_a	f_b	PR
I(0)	25,850	25,481	369	.009	.063	6.9
I(1)	27,273	27,085	188	.007	.025	3.6
I(2)	28,717	28,614	103	.004	.014	3.2
I(3)	30,164	30,121	43	.002	.007	3.2
I(4)	31,580	31,555	25	.001	.004	3.4
II	51,057	37,060	13,997	.313	.028	.09
III	44,365	43,996	369	.101	.183	1.8
IV	55,893	52,486	3,406	.097	.208	2.1

Table 14. TDM (HMO) vs. TDM (4-atom) calculations for the (001) face of anthracene at $295^{\circ}K$ (retarded field). All energies are in cm^{-1}. Oscillator strengths and polarization ratios are unitless.

TDM-SCF (static) $95^{o}K(001)$

Trans.	E_a	E_b	Sp	f_a	f_b	PR
I(0)	25,762	25,642	119	.010	.049	5.1
I(1)	27,214	27,154	60	.006	.025	4.0
I(2)	28,683	28,652	31	.004	.014	3.7
I(3)	30,150	30,137	12	.002	.006	3.6
I(4)	31,572	31,565	6	.001	.004	3.6
II	50,494	36,134	14,360	.359	.047	.13
III	44,675	44,453	222	.053	.171	3.2
IV	52,115	52,970	-854	.209	.260	1.2

Dipole (static)

Trans.	E_a	E_b	Sp	f_a	f_b	PR
I(0)	25,742	25,366	377	.012	.065	5.3
I(1)	27,199	27,045	155	.008	.045	2.7
I(2)	29,673	28,592	81	.005	.012	2.5
I(3)	30,144	30,111	34	.002	.006	2.5
I(4)	31,568	31,549	19	.001	.004	2.6
II	60,143	37,213	22,929	.346	.005	.02
III	43,822	44,035	-213	.105	.225	2.1
IV	51,511	52,398	-887	.161	.224	1.4

Table 15. TDM vs. Dipole calculations for the (001) face of anthracene at $95^{o}K$ (static field). All energies are in cm^{-1}. Oscillator strengths and polarization ratios are unitless.

TDM-SCF (retarded) $95^{o}K(001)$

Trans.	E_a	E_b	Sp	f_a	f_b	PR
I(0)	25,686	25,303	383	.013	.069	5.5
I(1)	27,170	27,028	142	.007	.021	2.9
I(2)	28,656	28,584	73	.004	.012	2.8
I(3)	30,138	30,108	30	.002	.006	2.8
I(4)	31,564	31,548	17	.001	.004	2.8
II	49,921	36,854	13,067	.301	.042	.14
III	44,403	43,927	476	.102	.186	1.8
IV	56,031	52,032	3,999	.116	.204	1.8

Dipole (retarded) $95^{o}K(001)$

Trans.	E_a	E_b	Sp	f_a	f_b	PR
I(0)	25,638	24,921	717	.017	.085	5.1
I(1)	27,141	26,939	202	.009	.017	1.9
I(2)	28,638	28,534	105	.005	.010	1.9
I(3)	30,129	30,084	44	.003	.005	1.9
I(4)	31,558	31,532	26	.002	.003	2.0
II	59,328	37,116	22,212	.178	.019	.1
III	43,087	43,279	192	.162	.223	1.4
IV	50,072	51,561	1,489	.168	.166	1.0

Table 16. TDM vs. Dipole calculations for the (001) face of anthracene at $95^{o}K$ (retarded field). All energies are in cm^{-1}. Oscillator strengths and polarization ratios are unitless.

TDM-SCF (static) $295^{o}K(20\bar{1})$

Trans.	E_a	E_b	Sp	f_a	f_b	PR
I(0)	25,880	25,670	211	.004	.047	11.0
I(1)	27,297	27,166	130	.004	.025	6.9
I(2)	28,733	28,658	75	.002	.014	5.7
I(3)	30,172	30,140	31	.001	.006	5.7
I(4)	31,584	31,567	18	.001	.004	5.4
II	39,053	37,009	2,044	1.318	.032	.02
III	45,329	44,475	854	.030	.173	5.8
IV	53,690	53,031	659	.005	.261	55.0

Dipole (static) $295^{o}K(20\bar{1})$

Trans.	E_a	E_b	Sp	f_a	f_b	PR
I(0)	25,922	25,413	509	.0007	.062	85
I(1)	27,239	27,059	269	.0005	.022	43
I(2)	28,752	28,599	154	.0003	.012	49
I(3)	30,179	30,113	66	.0001	.006	80
I(4)	31,588	31,550	38	.0000	.003	190
II	41,338	37,027	4,311	1.271	.013	.01
III	45,161	44,050	1,110	.133	.207	1.6
IV	53,728	52,475	1,253	.063	.224	3.5

Table 17. TDM vs. Dipole calculations for the $(20\bar{1})$ face of anthracene at $295^{o}K$ (static field). All energies are in cm^{-1}. Oscillator strengths and polarization ratios are unitless.

TDM-SCF (retarded) $295^{o}K(20\bar{1})$

Trans.	E_a	E_b	Sp	f_a	f_b	PR
I(0)	25,840	25,356	483	.012	.066	5.7
I(1)	27,265	27,044	221	.010	.022	2.1
I(2)	28,711	28,592	119	.008	.012	1.5
I(3)	30,160	30,112	49	.005	.006	1.1
I(4)	31,576	31,550	26	.005	.004	0.7
II	36,877	34,272	2,605	.037	1.139	31
III	45,277	43,907	1,370	.009	.180	19
IV	53,681	52,395	1,286	.003	.213	81

Dipole (retarded) $295^{o}K(20\bar{1})$

Trans.	E_a	E_b	Sp	f_a	f_b	PR
I(0)	25,916	25,012	904	.002	.081	53
I(1)	27,325	26,956	369	.001	.017	15
I(2)	28,750	28,543	207	.001	.010	16
I(3)	30,179	30,089	89	.0002	.005	24
I(4)	31,588	31,535	53	.0001	.003	48
II	36,974	36,705	269	.015	1.234	82
III	44,969	43,363	1,605	.027	.213	7.9
IV	53,610	51,930	1,679	.032	.179	5.6

Table 18. TDM vs. Dipole calculations for the $(20\bar{1})$ face of anthracene at $295^{o}K$ (retarded field). All energies are in cm^{-1}. Oscillator strengths and polarization ratios are unitless.

TDM-SCF (static) $295^{o}K(\bar{1}10)$

Trans.	E_{a*}	E_{b*}	Sp	f_{a*}	f_{b*}	PR
I(0)	26,108	25,706	401	.003	.017	5.1
I(1)	27,515	27,186	329	.004	.010	2.2
I(2)	28,882	28,668	214	.004	.006	1.4
I(3)	30,233	30,144	89	.002	.002	1.3
I(4)	31,616	31,569	47	.001	.002	1.3
II	37,619	37,204	415	.164	1.242	7.6
III	44,606	45,811	-1,205	.022	.069	3.1
IV	55,448	53,073	2,375	.083	.103	1.2

Dipole (static) $295^{o}K(\bar{1}10)$

Trans.	E_{a*}	E_{b*}	Sp	f_{a*}	f_{b*}	PR
I(0)	26,037	25,651	386	.004	.023	6.5
I(1)	27,430	27,153	278	.004	.012	2.8
I(2)	28,814	28,647	167	.004	.007	2.0
I(3)	30,202	30,133	68	.002	.003	1.9
I(4)	31,598	31,561	37	.001	.002	1.9
II	39,067	37,119	1,948	.005	1.248	265
III	45,906	44,800	1,107	.078	.193	2.5
IV	54,981	53,120	1,861	.068	.169	2.5

Table 19. TDM vs. Dipole calculations for the $(\bar{1}10)$ face of anthracene at $295^{o}K$ (static field). All energies are in cm^{-1}. Oscillator strengths and polarization ratios are unitless.

*Subscript b labels the energy and oscillator strength of the transition closest to the b crystal axis, while a labels the other.

TDM-SCF (retarded) 295°K($\bar{1}$10)

Trans.	E_{a*}	E_{b*}	Sp	f_{a*}	f_{b*}	PR
I(0)	26,090	25,599	491	.003	.022	6.4
I(1)	27,492	27,133	358	.005	.010	1.9
I(2)	28,860	28,640	221	.007	.006	.89
I(3)	30,220	30,132	88	.007	.003	.42
I(4)	31,599	31,560	39	.025	.005	.20
II	32,321	37,211	-4,890	1.161	.013	.01
III	44,370	45,749	-1,380	.017	.079	4.7
IV	55,263	52,796	2,467	.062	.014	1.7

Dipole (retarded) 295°K($\bar{1}$10)

Trans.	E_{a*}	E_{b*}	Sp	f_{a*}	f_{b*}	PR
I(0)	26,015	25,504	511	.005	.030	5.6
I(1)	27,403	27,087	316	.008	.013	1.7
I(2)	28,789	28,609	181	.008	.009	1.1
I(3)	30,188	30,114	74	.005	.005	1.0
I(4)	31,587	31,546	41	.005	.007	1.4
II	34,307	37,104	-2,798	.005	1.168	242
III	45,758	44,305	1,452	.032	.132	4.2
IV	54,833	52,710	2,117	.048	.136	2.9

Table 20. TDM vs. Dipole calculations for the ($\bar{1}$10) face of anthracene at 295°K (retarded field). All energies are in cm^{-1}. Oscillator strengths and polarization ratios are unitless.

*Subscript b labels the energy and oscillator strength of the transition closest to the b axis, while a labels the other.

TDM (static)			TDM (retarded)	
Trans.	θ_{a*}	θ_{b*}	θ_{a*}	θ_{b*}
I(0)	76.4	87.4	60.0	90.4
I(1)	73.6	85.6	51.8	87.9
I(2)	70.2	83.1	41.3	83.2
I(3)	65.7	79.7	28.4	71.7
I(4)	59.6	74.9	14.2	27.9
II	2.8	18.6	4.3	69.3
III	78.6	96.6	82.0	95.2
IV	102.2	101.0	102.7	96.4

Dipole (static)			TDM (retarded)	
Trans.	θ_{a*}	θ_{b*}	θ_{a*}	θ_{b*}
I(0)	59.1	72.9	40.0	68.1
I(1)	55.6	69.7	35.6	61.5
I(2)	51.6	65.8	31.3	52.3
I(3)	47.1	60.8	27.3	39.1
I(4)	41.6	54.8	24.5	22.4
II	1.2	72.8	3.3	106.0
III	164.7	132.7	148.6	116.8
IV	136.9	116.2	133.9	107.8

Table 21. Angles of the transition maximum on the $(\bar{1}10)$ face. Angles (in degrees) of the crystal transition moment measured clockwise from the projection of the C crystal axis in the $(\bar{1}10)$ plane of anthracene.

*Subscript b labels the energy and oscillator strength of the transition closest to the b crystal axis, while a labels the other.

Appendix A

Anthracene and Tetracene: Crystal and Molecular Data

I. Anthracene

Anthracene forms monoclinic crystals with space group P_{2_1}/a (C_{2h}^5) with two molecules per unit cell. The unit cell dimensions at 295°K are:[23] a = 8.561, b = 6.036, c = 11.163 Å, and $\beta = 124°42'$. At 95°K the unit cell dimenstions[46] contract to a = 8.443, b = 6.002, c = 11.124 Å, and $\beta = 125°36'$.

The molecular data employed was the same as Philpott's[31] to facilitate comparisons of the two calculations. The transition frequencies (ω in cm^{-1}) and the transition moment lengths (μ in Å) were: $\omega_{I(n)} = 26{,}000 + n1400$, $\mu_{total} = .61$, and Franck-Condon factors[47] $\xi^2_{I(n)} = 0.324, 0.316, 0.218, 0.092, 0.050$ for n = 0, ... , 4; $\omega_{II} = 39{,}000$, $\mu_{II} = 1.87$; $\omega_{III} = 45{,}200$, $\mu_{III} = .64$; $\omega_{IV} = 54{,}000$, $\mu_{IV} = .83$.

II. Tetracene

Tetracene[24] forms triclinic crystals with space group P_1 and unit cell dimensions: a = 7.98, b = 6.14, c = 13.57 Å; $\alpha = 101.3°$, $\beta = 113.2°$, and $\gamma = 87.5°$.

The molecular data was taken to be (following Philpott[31]) a series of five transitions (ω in cm^{-1} and μ in Å): $\omega_{I(n)} = 22{,}220 + n1430$, $\mu_{total} = .6$Å, and Franck-Condon factors[48] $\xi^2_{I(n)} = 0.271, 0.327, 0.209, 0.134, 0.060$ for n = 0, ... , 4; $\omega_{II} = 35{,}030$, $\mu_{II} = .46$; $\omega_{III} = 38{,}850$, $\mu_{III} = 1.88$; $\omega_{IV} = 44{,}000$; $\mu_{IV} = 1.03$; $\omega_V = 49{,}000$; $\mu_V = .97$.

Appendix B

Planewise Dipole Sums: Long Range Terms

In the point-dipole approximation, the static long range interactions may be evaluated as an integral over a continuous planar dipole medium. When there are only two molecules per unit cell, as in the systems studied here, the plane may be chosen such that the integral can be taken over a single plane which includes the line connecting the two point dipoles in the same unit cell. The wavevector (k) is chosen normal to the plane which allows the projection of the dipole in the plane to be written as the magnitude of the dipole moment (μ) multiplied by the sine of the angle between the wavevector and the dipole vector:

$$P = \mu \sin(k\mu). \qquad (B.1)$$

Then if the polar axis is chosen as the direction of the dipole projection in the plane, the angle between $\vec{R}$ and the dipole projection is the polar angle, ϕ, and the static dipole sum (in the plane)

$$E = \vec{\mu}_i \sum_j e^{ik \cdot R_j} \left[\frac{1 - 3\hat{R}\hat{R}}{R^3} \right] \vec{\mu}_j \qquad (B.2)$$

can be expressed as the integral over a continuous density ($\frac{\mu}{A}$):

$$E = \frac{\mu^2}{A} \int_{R_0}^{R_f} \int_0^{2\pi} \frac{1-3P^2 \cos^2\phi}{R^3} R \, dR \, d\phi \qquad (B.3)$$

where $e^{ik \cdot R_j} = 1$ (since k is normal to the plane), and A is the area of a two dimensional unit cell in the plane. The integral in (B.3) is over an annular area with an inner radius R_0 and an outer radius R_f.

Integration over ϕ gives

$$E = \frac{2 \Pi \mu^2}{A} \int_{R_0}^{R_f} \frac{1 - 3/2\ P^2}{R^2}\ dR \qquad (B.4)$$

Then integrating (B.4) over R yields

$$E = \frac{2 \Pi \mu^2}{A} \left[\frac{3/2\ P^2 - 1}{R} \right]_{R_0}^{R_f} , \qquad (B.5)$$

and substituting

$$\frac{3}{2} P^2 = \frac{3}{2} \sin^2 (k\mu) = \frac{3}{2} - \frac{3}{2} \cos^2 (k\mu) \qquad (B.6)$$

in (B.5) gives, after rearranging, equation (3.14):

$$E = \frac{\Pi \mu^2}{A} [3 \cos (k\ ) - 1\ ] \left[\frac{1}{R_0} - \frac{1}{R_f} \right] . \qquad (B.7)$$

Appendix C

Latisum V

Latisum V is the fifth in a series of computer programs of increasing sophistication developed in the course of this study. All data reported in the main text were obtained from this final version. The language is Fortran IV.

```
      DIMENSION CXC(6),CYC(6),CZC(6),DCX(6,4),DCY(6,4),DCZ(6,4),Q(6,4)
     1,XDIP(6,4),YDIP(6,4),ZDIP(6,4),VSUM(8,6,32),V( 8,6,32),FINK(6,4),
     2X(4,30),Y(4,30),Z(4,30),CH(6,4,30),VZUM(8,6,32),CHONK(6),
     3 XON(6),YON(6),ZON(6),XAD(6),YAD(6),ZAD(32),TITLE(20),TRANS(6),
     4ENT(6),INV(6),EUM(6,6),EMM(6,6,6),CHUD(6,6),DDDZ(32),XD(32),
     5YD(32),ZD(32),VIB(6,6),EVIB(6,6),HS(32,32),HZ(32,32),JFA(10),
     6JFB(10),HHD(4,4,6,6),HHP(4,4,6,6),UZ(32,32),US(32,32),ZR(32),
     7XPZ(32),YPZ(32),ZPZ(32),XPS(32),YPS(32),ZPS(32)
      COMMON XD,YD,ZD,DLX,DLY,DLZ,D1X,D1Y,D1Z
    1 READ(5,2)N,NAT,NT,NIX,JH,IFF,JERI,MG
    2 FORMAT(10I3)
      IF(N)444,328,5001
 5001 READ(5,3) ALFA,BATA,GAMA,AA,BB,CC
      UT4=0.0
      UT7=0.0
      UT8=0.0
      UT1= AA
      GAMA=GAMA/57.29578
      BATA=BATA/57.29578
      ALFA=ALFA/57.29578
      UT2=BB*COS(GAMA)
      UT3=CC*COS(BATA)
      UT5=BB*SIN(GAMA)
      UT6=CC*(COS(ALFA)-COS(BATA)*COS(GAMA))/SIN(GAMA)
      VOL=AA*BB*CC*(SQRT(1.0-COS(ALFA)*COS(ALFA)-COS(BATA)*COS(BATA)-
     1COS(GAMA)*COS(GAMA)+2.0*COS(ALFA)*COS(BATA)*COS(GAMA)))
      UT9=VOL/(AA*BB*SIN(GAMA))
      DO 410 K=1,N
      US(1,K)=0.0
      READ(5,3)XON(K),YON(K),ZON(K),XAD(K),YAD(K),ZAD(K),CHONK(K)
      READ(5,405)GGX,GGY,GGZ
  405 FORMAT (3F10.5)
      CXC(K)=UT1*GGX+UT2*GGY+UT3*GGZ
      CYC(K)=UT5*GGY+UT6*GGZ
  410 CZC(K)=UT9*GGZ
      DO 470 I=1,NAT
```

```
      READ(5,3) WOX,WOY,WOZ
      DO 470 K=1,N
      WWX=XON(K)*WOX+XAD(K)
      WWY=YON(K)*WOY+YAD(K)
      WWZ=ZON(K)*WOZ+ZAD(K)
      IF(K-1)1337,1337,1338
1337  WOX=WWX
      WOY=WWY
      WOZ=WWZ
1338  CONTINUE
      X(K,I)=UT1*WWX+UT2*WWY+UT3*WWZ
      Y(K,I)=UT5*WWY+UT6*WWZ
 470  Z(K,I)=UT9*WWZ
      DO 490 L=1,NT
      READ(5,3)(CH(L,1,IT),IT=1,NAT)
      READ(5,3) TRANS(L),ENT(L)
      TRANS(L)=SQRT(TRANS(L)/(.00047*ENT(L)))
      IF(JERI)1013,1013,1014
1014  SXO=0.0
      SYO=0.0
      SZO=0.0
      DO1018JA=1,NAT
      SXO=SXO+CH(L,1,JA)*X(1,JA)
      SYO=SYO+CH(L,1,JA)*Y(1,JA)
1018  SZO=SZO+CH(L,1,JA)*Z(1,JA)
      BARF=SXO*SXO+SYO*SYO+SZO*SZO
      BNNP=SQRT(BARF)
      FRAB=TRANS(L)/BNNP
      CKX=SXO/BNNP
      CKY=SYO/BNNP
      CKZ=SZO/BNNP
1022  DO1019KA=1,NAT
1019  CH(L,1,KA)=CH(L,1,KA)*FRAB
1013  DO 490 K=1,N
      IF(ZAD(K)-2.0)9222,9222,9224
9224  DO 9470 I=1,NAT
```

```
      READ(5,3)WOX,WOY,WOZ
      X(K,I)=WOX*UT1+WOY*UT2+WOZ*UT3
      Y(K,I)=WOY*UT5+WOZ*UT6
9470  Z(K,I)=WOZ*UT9
      ZAD(K)=0.0
9222  IF( CHONK(K)-1.0 ) 2222,2222,2244
2244  READ(5,3) (CH(L,K,IT),IT=1,NAT)
      GO TO 490
2222  DO 9490 I=1,NAT
      CH(L,K,I)=CHONK(K)*CH(L,1,I)
9490  CONTINUE
 490  CONTINUE
      WRITE(6,946)
 946  FORMAT(1H1)
      WRITE(6,7003) UT1,UT2,UT3,UT4,UT5,UT6,UT7,UT8,UT9,VOL
7003  FORMAT(///,' TRANSFORMATION MATRIX',//,9F10.5,' VOL=',F12.5)
      DO 1199 IZ=1,N
      WRITE(6,1101)IZ
1101  FORMAT(1X,'MOLECULE NO.',I3)
      WRITE(6,1201)
1201  FORMAT(1X,' ATOM NO.',4X,' X',10X,' Y',10X,' Z',9X,' T1',9X,
     1 ' T2',9X,' T3',9X,' T4',9X,' T5',9X,' T6')
      DO 1199 IY=1,NAT
      WRITE(6,1102) IY,X(IZ,IY),Y(IZ,IY),Z(IZ,IY), (CH(IX,IZ,IY),
     1IX=1,NT)
1102  FORMAT(3X,I3,3X,9(F10.5,2X))
1199  CONTINUE
      WRITE(6,2123)
      WRITE(6,4042)
4042  FORMAT( ' TRANS. NO.',3X,' MOL.NO.',3X,' TRANS. MOM.',3X, ' DIR.
     1 COS.  X',13X,' Y',14X,' Z',8X,' ABS(M(1)*M(N))')
      DO 4005 K=1,NT
      DO 4005 I=1,N
      SXO=0.0
      SYO=0.0
      SZO=0.0
```

```
      DO 4048 JA=1,NAT
      SXO=SXO+CH(K,I,JA)*X(I,JA)
      SYO=SYO+CH(K,I,JA)*Y(I,JA)
4048  SZO=SZO+CH(K,I,JA)*Z(I,JA)
      BARF=SXO*SXO+SYO*SYO+SZO*SZO
      BNNP= SQRT( BARF )
      Q(K,I)=BNNP
      DCX(K,I)=SXO/BNNP
      DCY(K,I)=SYO/BNNP
      DCZ(K,I)=SZO/BNNP
      XDIP(K,I)=DCX(K,I)*Q(K,I)
      YDIP(K,I)=DCY(K,I)*Q(K,I)
      ZDIP(K,I)=DCZ(K,I)*Q(K,I)
      FINK(K,I)=DCX(K,I)*DCX(K,1)+DCY(K,I)*DCY(K,1)+DCZ(K,I)*DCZ(K,1)
      WRITE(6,4047)K,I,Q(K,I),DCX(K,I),DCY(K,I),DCZ(K,I),FINK(K,I)
4047  FORMAT(4X,I3,8X,I3,13X,F10.6,4(6X,F10.6))
4005  CONTINUE
 444  READ(5,445) LH,LK,LL,RMIN,RMAX,RCHK,SMH,SMK,SML,INK
 445  FORMAT(3I3,6F10.5,2I3)
      SML=SML-1.0
      SMK=SMK-1.0
      IF(N)220,328,210
 220  N=-N
 210  IF(IFF)401,401,6
   6  READ(5,3)UXX,UYY,UZZ,UXY,UXZ,UYZ,GEN
   3  FORMAT(8F10.5)
      IBB=1
      GO TO 187
 401  GEN=1.0
      UXX=1.0
      UYY=1.0
      UZZ=1.0
      UXY=1.0
      UXZ=1.0
      UYZ=1.0
      IF(NIX) 191,192,192
```

```
  191 IBB=0
      GO TO 187
  192 IBB=1
  187 CONTINUE
      WRITE(6,109)  RMIN,RMAX
  109 FORMAT(1X,'RMIN=',F6.3,6X,'RMAX=',F6.3)
 7000 READ(5,7010)IDK,I7,I8K,DLH,DLK,DLL,D2X,D2Y,D2Z
 7010 FORMAT(3I3,6F10.5)
      READ(5,3001)TITLE
 3001 FORMAT(20A4)
      IF(I7)1,7011,7011
 7011 LU=0
      KU=0
      IF(DLH)701,702,701
  702 KU=KU+1
      XON(KU)=UT1
      YON(KU)=0.0
      ZON(KU)=0.0
      GO TO 710
  701 LU=LU+1
      XAD(LU)=UT1/DLH
      YAD(LU)=0.0
      ZAD(LU)=0.0
  710 IF(DLK) 711,712,711
  712 KU=KU+1
      XON(KU)=UT2
      YON(KU)=UT5
      ZON(KU)=0.0
      GO TO 720
  711 LU=LU+1
      XAD(LU)=UT2/DLK
      YAD(LU)=UT5/DLK
      ZAD(LU)=0.0
  720 IF(DLL) 721,722,721
  722 KU=KU+1
      XON(KU)=UT3
```

```
      YON(KU)=UT6
      ZON(KU)=UT9
      GO TO 730
  721 LU=LU+1
      XAD(LU)=UT3/DLL
      YAD(LU)=UT6/DLL
      ZAD(LU)=UT9/DLL
  730 IF(KU-1) 740,750,760
  740 XON(1)=XAD(3)-XAD(1)
      YON(1)=YAD(3)-YAD(1)
      ZON(1)=ZAD(3)-ZAD(1)
  750 XON(2) = XAD(2) - XAD(1)
      YON(2) = YAD(2) - YAD(1)
      ZON(2) = ZAD(2) - ZAD(1)
  760 TX=YON(1)*ZON(2)-YON(2)*ZON(1)
      TY=ZON(1)*XON(2)-ZON(2)*XON(1)
      TZ=XON(1)*YON(2)-XON(2)*YON(1)
      ZAP=SQRT(TX*TX+TY*TY+TZ*TZ)
      DLX=TX/ZAP
      DLY=TY/ZAP
      DLZ=TZ/ZAP
      IF(I8K+1)7842,7843,7841
 7843 D3X=DLX
      D3Y=DLY
      D3Z=DLZ
      D3H=DLH
      D3K=DLK
      D3L=DLL
      DLH=D2X
      DLK=D2Y
      DLL=D2Z
      I8K=-3
      GO TO 7011
 7842 D2X=DLX
      D2Y=DLY
      D2Z=DLZ
```

```
      DLX=D3X
      DLY=D3Y
      DLZ=D3Z
      DLH=D3H
      DLK=D3K
      DLL=D3L
      GO TO 7833
7841  IF(I8K-1) 7821,7833,7834
7821  T33=SQRT(XON(1)*XON(1)+YON(1)*YON(1)+ZON(1)*ZON(1))
      D1X=XON(1)/T33
      D1Y=YON(1)/T33
      D1Z=ZON(1)/T33
      GO TO 7824
7834  D1X=D2X
      D1Y=D2Y
      D1Z=D2Z
      T33=SQRT(D1X*D1X+D1Y*D1Y+D1Z*D1Z)
      D1X=D1X/T33
      D1Y=D1Y/T33
      D1Z=D1Z/T33
      GO TO 7824
7833  D1X=DLY*D2Z-DLZ*D2Y
      D1Y=DLZ*D2X-DLX*D2Z
      D1Z=DLX*D2Y-DLY*D2X
      T33=SQRT(D1X*D1X+D1Y*D1Y+D1Z*D1Z)
      D1X=D1X/T33
      D1Y=D1Y/T33
      D1Z=D1Z/T33
7824  DO 8671 K=1,NT
      DO 8671 I = 1,N
8671  EUM(K,I) = XDIP(K,I) * DLX + YDIP(K,I) * DLY + ZDIP(K,I) * DLZ
8000  QN=0.0004703/N
      DO 446 K=1,NT
      DO 446 J=1,NT
      CHUD(K,J)=0.0
      DO 446 I=1,N
```

```
      VZUM(I,K,J)=0.0
      VSUM(I,K,J)=0.0
      HHD(4,I,K,J)=0.0
  446 HHP(4,I,K,J)=0.0
      IF(IOK+5)813,818,813
  813 ND=0
 8002 DO 8301 J=1,NT
      READ(5,8001) NLEV
 8001 FORMAT(8I3)
      IF(NLEV) 8331,8331,8333
 8331 INV(J)=1
      EVIB(J,1)=ENT(J)
      VIB(J,1)=1.0
      NLEV=1
      GO TO 8301
 8333 INV(J)=NLEV
      READ(5,8003) ( VIB(J,K),K=1,NLEV)
      READ(5,8003) (EVIB(J,K),K=1,NLEV)
 8003 FORMAT(8F10.5)
      DO 8035 L=1,NLEV
 8035 VIB(J,L)=SQRT(VIB(J,L))
 8301 ND=ND+NLEV
  818 IZI=0
  351 DO 830 IR=1,N
      DO 828 KE=1,NT
      DO 828 LE=1,NT
      DO 828 IE=1,N
  828 EMM(KE,LE,IE)=XDIP(KE,IR)*XDIP(LE,IE)+YDIP(KE,IR)*YDIP(LE,IE)+
     1ZDIP(KE,IR)*ZDIP(LE,IE)
      IF(IOK)891,599,894
  891 IF(IOK+3)3893,881,882
  882 IZI=1
      IF(IR-1)881,881,895
  881 IF(NIX)883,883,884
  883 DO 873 I1=1,N
      DO 873 I2=1,NT
```

```
      READ(5,3) (VZUM(I1,I2,I3),I3=1,NT)
      DO 873 I4=1,NT
  873 HHP(IR,I1,I2,I4)=VZUM(I1,I2,I4)
      GO TO 3895
 3893 DO 3896 J1=1,N
      DO 3896 J2=1,NT
      DO 3896 J4=1,NT
 3896 VZUM(J1,J2,J4)=HHP(IR,J1,J2,J4)
 3895 IF(NIX)895,884,884
  884 IF(IOK+3)3874,3884,3884
 3874 DO 3875 J1=1,N
      DO 3875 J2=1,NT
      DO 3875 J4=1,NT
 3875 VSUM(J1,J2,J4)=HHD(IR,J1,J2,J4)
      GO TO 895
 3884 DO 876 I1=1,N
      DO 876 I2=1,NT
      READ(5,3) (VSUM(I1,I2,I3),I3=1,NT)
      DO 876 I4=1,NT
  876 HHD(IR,I1,I2,I4)=VSUM(I1,I2,I4)
      GO TO 895
  894 IZI=1
      IF(IR-1)592,592,895
  599 DO 773 K=1,NT
      DO 773 J=1,NT
      CHUD(K,J)=0.0
      DO 773 I=1,N
      VSUM(I,K,J)=0.0
      VZUM(I,K,J)=0.0
      HHD(4,I,K,J)=0.0
  773 HHP(4,I,K,J)=0.0
      IF(IR-1)592,592,7001
  592 WRITE(6,7822)
 7822 FORMAT(1H1,10X,' CONVERGENCE TEST MATRICES'///)
 7001 VH=SMH
      C1X=CXC(IR)
```

```
      C1Y=CYC(IR)
      C1Z=CZC(IR)
      DO 50 IS=1,LH
      VL=SML
      VK=SMK
      DO 40 JJ=1,LK
      VK=VK+1.0
      DO 30 KK=1,LL
      VL=VL+1.0
      RX=UT1*VH+UT2*VK+UT3*VL
      RY=UT5*VK+UT6*VL
      RZ=UT9*VL
      DO 30 I=1,N
      RRX=RX+CXC(I)-C1X
      RRY=RY+CYC(I)-C1Y
      RRZ=RZ+CZC(I)-C1Z
      R=SQRT(RRX*RRX+RRY*RRY+RRZ*RRZ)
      IF(RMIN+.001-R)108,30,30
  108 IF(RMAX-R)30,104,104
  104 IF(IBB) 502,502,101
  101 IF (ABS(RRX)-0.1) 71,70,70
   71 IF (ABS(RRY)-0.1) 73,72,72
   73 IF (ABS (RRZ)-0.1) 98,74,74
   72 IF (ABS(RRZ)-0.1) 76,75,75
   70 IF (ABS(RRY)-0.1) 78,77,77
   78 IF (ABS(RRZ)-0.1) 80,79,79
   77 IF (ABS (RRZ)-0.1) 81,88,88
   98 GO TO 30
   74 FF=UZZ
      KOK=2
      GO TO 582
   75 FF=UYZ
      KOK=1
      GO TO 582
   76 FF=UYY
      KOK=3
```

```
      GO TO 582
   79 FF=UXZ
      KOK=1
      GO TO 582
   80 FF=UXX
      KOK=4
      GO TO 582
   81 FF=UXY
      KOK=5
      GO TO 582
   88 FF=GEN
      KOK=1
      GO TO 592
  502 FF=1.0
  582 IF(NIX) 574,574,110
  574 DO 211 J=1,NAT
      BRX=RX+X(I,J)
      BRY=RY+Y(I,J)
      BRZ=RZ+Z(I,J)
      DO 211 L=1,NAT
      XAX=BRX-X(IR,L)
      YAY=BRY-Y(IR,L)
      ZAZ=BRZ-Z(IR,L)
      ROPE=SQRT(XAX*XAX+YAY*YAY+ZAZ*ZAZ)
      DO 211 IPT=1,NT
      DO 211 JPT=1,NT
  211 CHUD(IPT,JPT)=CHUD(IPT,JPT)+CH(IPT,IR,L)*CH(JPT,I,J)/ROPE
      DO 673 MPT=1,NT
      DO 673 NPT=1,NT
      VZUM(I,MPT,NPT)=VZUM(I,MPT,NPT)+CHUD(MPT,NPT)*FF/0.1986
      IF(R-RCHK)673,673,7773
 7773 HHP(4,I,MPT,NPT)=HHP(4,I,MPT,NPT)+CHUD(MPT,NPT)*FF/0.1986
  673 CHUD(MPT,NPT)=0.0
      IF(NIX) 30,110,110
  110 DCRX=RRX/R
      DCRY=RRY/R
```

```
      DCRZ=RRZ/R
      DO 155 K=1,NT
      GO TO(160,174,176,180,181),KOK
  160 YM1=0.0
      APE=DCY(K,IR)*DCRZ-DCZ(K,IR)*DCRY-(DCRX*DCX(K,IR)*DCRY-DCRX*DCRX*
     1DCY(K,IR))/DCRZ
      BUM=DCZ(K,IR)*DCRX-DCX(K,IR)*DCRZ-(DCRY*DCRY*DCX(K,IR)-DCY(K,IR)*
     1DCRX*DCRY)/DCRZ
      COP=(DCRY*APE/BUM-DCRX)/DCRZ
      DCXX=1.0/SQRT(1.0+APE*APE/(BUM*BUM)+COP*COP)
      DCXY=-DCXX*APE/BUM
      DCXZ=COP*DCXX
      XM1=DCXX*XDIP(K,IR)+DCXY*YDIP(K,IR)+DCXZ*ZDIP(K,IR)
      ZM1=DCRX*XDIP(K,IR)+DCRY*YDIP(K,IR)+DCRZ*ZDIP(K,IR)
      GO TO 230
  174 XM1=XDIP(K,IR)
      YM1=YDIP(K,IR)
      ZM1=ZDIP(K,IR)
      GO TO 230
  176 XM1=XDIP(K,IR)
      YM1=ZDIP(K,IR)
      ZM1=YDIP(K,IR)
      GO TO 230
  180 XM1=ZDIP(K,IR)
      YM1=YDIP(K,IR)
      ZM1=XDIP(K,IR)
      GO TO 230
  181 YM1=0.0
      AIR=(ZDIP(K,IR)*(DCRY*DCRY/DCRX+DCRX))/(DCRX*YDIP(K,IR)-
     1XDIP(K,IR)*DCRY)
      BAR=-DCRY/DCRX
      DCXY=1.0/SQRT(1.0+AIR*AIR+BAR*BAR)
      DCXX=BAR*DCXY
      DCXZ=AIR*DCXY
      XM1=DCXX*XDIP(K,IR)+DCXY*YDIP(K,IR)+DCXZ*ZDIP(K,IR)
      ZM1=DCRX*XDIP(K,IR)+DCRY*YDIP(K,IR)+DCRZ*ZDIP(K,IR)
```

```
230 DO 155 L=1,NT
    GO TO (260,274,276,280,281),KOK
260 YM2=0.0
    XM2=DCXX*XDIP(L,I)+DCXY*YDIP(L,I)+DCXZ*ZDIP(L,I)
    ZM2=DCRX*XDIP(L,I)+DCRY*YDIP(L,I)+DCRZ*ZDIP(L,I)
    GO TO 231
274 XM2=XDIP(L,I)
    YM2=YDIP(L,I)
    ZM2=ZDIP(L,I)
    GO TO 231
276 XM2=XDIP(L,I)
    YM2=ZDIP(L,I)
    ZM2=YDIP(L,I)
    GO TO 231
280 XM2=ZDIP(L,I)
    YM2=YDIP(L,I)
    ZM2=XDIP(L,I)
    GO TO 231
281 YM2=0.0
.   XM2=DCXX*XDIP(L,I)+DCXY*YDIP(L,I)+DCXZ*ZDIP(L,I)
    ZM2=DCRX*XDIP(L,I)+DCRY*YDIP(L,I)+DCRZ*ZDIP(L,I)
231 DUMDUM=(XM1*XM2+YM1*YM2- 2.0*ZM1*ZM2)/(R*R*R)
    IF(R-RCHK)155,155,7771
7771 HHD(4,I,K,L)=HHD(4,I,K,L)+DUMDUM*FF/0.1986
155 VSUM(I,K,L)=VSUM(I,K,L)+DUMDUM*FF/0.1986
 30 CONTINUE
 40 VL=SML
 50 VH=VH+1.0
598 IF(NIX)854,854,852
854 DO 853 I1=1,N
    WRITE(6,682)IR,I1
    DO 853 I2=1,NT
    WRITE(6,683) I2,(HHP(4,I1,I2,I6),I6=1,NT)
    DO 853 I3=1,NT
853 HHP(IR,I1,I2,I3)=VZUM(I1,I2,I3)
    IF(NIX)895,852,852
```

```
852 DO 856 I1=1,N
    WRITE(6,692)IR,I1
    DO 856 I2=1,NT
    WRITE(6,683) I2,(HHD(4,I1,I2,I6),I6=1,NT)
    DO 856 I3=1,NT
856 HHD(IR,I1,I2,I3)=VSUM(I1,I2,I3)
895 DO 830 IC=1,N
857 IH=IC
    IF(IZI)859,859,858
858 IF(IR-1)859,859,868
868 AX=CXC(IR)-CXC(IC)
    AY=CYC(IR)-CYC(IC)
    AZ=CZC(IR)-CZC(IC)
    AX=AX*AX+AY*AY+AZ*AZ
    AX=SQRT(AX)
    AJ=0.005
823 DO 829 IA=1,N
    AY=CXC(IA)*CXC(IA)+CYC(IA)*CYC(IA)+CZC(IA)*CZC(IA)
    AY=SQRT(AY)
    IF(ABS(AX-AY)-AJ)835,835,829
835 AMM=ABS(EMM(1,1,IC)/(Q(1,IC)*Q(1,IR)))
    AZ=ABS(ABS(FINK(1,IA))-AMM)
    IF(AZ-AJ)825,825,829
825 IH=IA
    GO TO 824
829 CONTINUE
    AJ=AJ+0.005
    GO TO 823
824 IF(AJ-0.1)837,837,836
836 WRITE(6,838)IR,IC
838 FORMAT(10X,' NO INTERACTION ANALOG EXISTS FOR ELEMENT(',2I3,' )',
   1//,20X,' STANDARD FIXUP TAKEN',//)
    IF (IOK)328,328,860
860 IOK=0
    IZI=0
    GO TO 599
```

```
 837 US(IR,IC)=AJ
     IF(NIX)501,501,503
 501 DO 504 I1=1,NT
     DO 504 I2=1,NT
 504 HHP(IR,IC,I1,I2)=VZUM(IH,I1,I2)
 562 IF(NIX)859,503,503
 503 DO 505 I1=1,NT
     DO 505 I2=1,NT
 505 HHD(IR,IC,I1,I2)=VSUM(IH,I1,I2)
 859 JR=(IR-1)*ND
     KO2=(IR-1)*N+IC
     IF(I7)5733,5733,7216
5733 DO 5744 K=1,NT
     DO 5744 L=1,NT
5744 V(K,L,KO2)=0.0
     GO TO 7214
7216 DO 7217 K=1,NT
     DO 7217 L=1,NT
5930 VIF=12.56637*(EUM(K,IR)*EUM(L,IC)-EMM(K,L,IC)/3.0)/(VOL*0.1986)
     IF(I7-1)7217,7217,832
 832 VIF=1.25*VIF-EMM(K,L,IC)*2.0944/(VOL*0.1986)
7217 V(K,L,KO2)=VIF
7214 DO 830 K=1,NT
     IP=INV(K)
     DO 830 KK=1,IP
     JR=JR+1
     JC=(IC-1)*ND
     DO 830 L=1,NT
     IF(I7)5831,5831,7830
5831 AAZ=VZUM(IH,K,L)
     AAS=VSUM(IH,K,L)
     GO TO 5832
7830 VIF=V(K,L,KO2)
 831 AAZ=VZUM(IH,K,L)+VIF
     AAS=VSUM(IH,K,L)+VIF
5832 IB=INV(L)
```

```
      DO 830 L6=1,IB
      JC=JC+1
      IF(JC-JR)843,844,843
  843 AAV=VIB(K,KK)*VIB(L,L6)
      HZ(JR,JC)=AAZ*AAV
      HS(JR,JC)=AAS*AAV
      GO TO 830
  844 AAV=VIB(L,L6)
      SE=EVIB(L,L6)
      HZ(JR,JR)=AAZ*AAV*AAV+SE
      HS(JR,JR)=AAS*AAV*AAV+SE
      BX=XDIP(K,IR)*AAV
      BY=YDIP(K,IR)*AAV
      BZ=ZDIP(K,IR)*AAV
      XD(JR)=BX
      YD(JR)=BY
      ZD(JR)=BZ
      DDDZ(JR)=SE
      IF(IR-1)830,511,830
  511 ZAD(JR)=AAV*AAV*SE*TRANS(L)*TRANS(L)*0.0004703
  830 CONTINUE
      IF(I7-1)602,7606,7602
 7602 WRITE(6,7603)
 7603 FORMAT(1H1,10X,' LONG RANGE INTS.--RETARDED'///)
      GO TO 7607
 7606 WRITE(6,7608)
 7608 FORMAT(1H1,10X,' LONG RANGE INTS.--  STATIC'///)
 7607 DO 7609 IR=1,N
      JR=(IR-1)*N
      DO 7609 IC=1,N
      KO2=JR+IC
      WRITE(6,692) IR,IC
      DO 7609 K1=1,NT
 7609 WRITE(6,683)K1,(V(K1,K2,KO2),K2=1,NT)
  602 WRITE(6,681) IOK
  681 FORMAT(1H1,10X,' ONE SITE INTERACTION MATRICES ( LATTICE SUM ONLY
```

```
   1)',10X,' IOK=',I3,//)
     IF(NIX)603,603,604
 603 DO 620 IR=1,N
     DO 620 IC=1,N
     WRITE(6,682)IR,IC
 682 FORMAT(//,'  PT CH MATRIX(',I2,I3,' )'/15X,' 1',9X,' 2',9X,' 3',
    19X,' 4',9X,' 5',9X,' 6'/)
     DO 620 JR=1,NT
     WRITE(6,683)JR,(HHP(IR,IC,JR,JC),JC=1,NT)
 683 FORMAT(2X,I3,5X,6F11.6)
     IF(MG)620,620,621
 621 WRITE(7,3) (HHP(IR,IC,JR,
 620 CONTINUE
     IF(NIX)605,604,604
 604 DO 630 IR=1,N
     DO 630 IC=1,N
     WRITE(6,692)IR,IC
 692 FORMAT(//,' DIPOLE MATR                                    9X,' 3',
    19X,' 4',9X,' 5',9X,' 6'
     DO 630 JR=1,NT
     WRITE(6,683)JR,(HHD(IR,IC
     IF(MG)630,630,631
 631 WRITE(7,3) (HHD(IR,IC,JR,JC),
 630 CONTINUE
 605 IF(IZI)601,601,606
 606 WRITE(6,614)
 614 FORMAT(////,' INCOMPATABILITY MATRIX')
     DO 607 IR=1,N
 607 WRITE(6,2299) (US(IR,IC),IC=1,N)
2299 FORMAT(1X,8F10.5)
 601 II=N*ND
     DO 9901 I=1,II
     DO 9901 J=1,II
     IF(I-J)9902,9903,9902
9903 UZ(I,I)=1.0
     US(I,I)=1.0
```

```
      GO TO 9901
 9902 UZ(I,J)=0.0
      UZ(J,I)=0.0
      US(I,J)=0.0
      US(J,I)=0.0
 9901 CONTINUE
      IF(NIX)9002,9002,9003
 9002 WRITE(6,947) TITLE
      IF(II-16)9406,9406,9409
 9406 DO 9407 I=1,II
 9407 WRITE(6,9408) (HZ(I,J),J=1,II)
 9408 FORMAT(2X,16F8.4)
      GO TO 9410
 9409 DO 9419 I=1,II
      WRITE(6,9418) I
 9418 FORMAT(2X,' ROW(',I2,' )')
 9419 WRITE(6,9408) (HZ(I,J),J=1,II)
 9410 DO 9004 M=1,II
 9004 ZR(M)=HZ(M,M)
      IM=II-1
      DO 9005 I=1,IM
      IN=I+1
      DO 9005 J=IN,II
      IF(ABS(ZR(I)-ZR(J))-0.001) 9006,9005,9005
 9006 HIJ=HZ(I,J)
      HII=HZ(I,I)
      HJJ=HZ(J,J)
      HD=ABS(HII-HJJ)
      IF(HD-0.001)9013,9013,9012
 9013 HDG=2.0
      GO TO 9014
 9012 HDG=SIGN(2.0,(HII-HJJ))
 9014 TG=HDG*HIJ/(HD+SQRT(HD*HD+4.*HIJ*HIJ))
      CO=1.0/SQRT(1.+TG*TG)
      SN=TG*CO
      HZ(I,I)=CO*CO*(HII+TG*(2.*HIJ+TG*HJJ))
```

```
   1)',10X,' IOK=',I3,//)
     IF(NIX)603,603,604
603  DO 620 IR=1,N
     DO 620 IC=1,N
     WRITE(6,682)IR,IC
682  FORMAT(//,'  PT CH MATRIX(',I2,I3,' )'/15X,' 1',9X,' 2',9X,' 3',
    19X,' 4',9X,' 5',9X,' 6'/)
     DO 620 JR=1,NT
     WRITE(6,683)JR,(HHP(IR,IC,JR,JC),JC=1,NT)
683  FORMAT(2X,I3,5X,6F11.6)
     IF(MG)620,620,621
621  WRITE(7,3) (HHP(IR,IC,JR,JC),JC=1,NT)
620  CONTINUE
     IF(NIX)605,604,604
604  DO 630 IR=1,N
     DO 630 IC=1,N
     WRITE(6,692)IR,IC
692  FORMAT(//,' DIPOLE MATRIX(',I2,I3,' )'/15X,' 1',9X,' 2',9X,' 3',
    19X,' 4',9X,' 5',9X,' 6'/)
     DO 630 JR=1,NT
     WRITE(6,683)JR,(HHD(IR,IC,JR,JC),JC=1,NT)
     IF(MG)630,630,631
631  WRITE(7,3) (HHD(IR,IC,JR,JC),JC=1,NT)
630  CONTINUE
605  IF(IZI)601,601,606
606  WRITE(6,614)
614  FORMAT(////,' INCOMPATABILITY MATRIX')
     DO 607 IR=1,N
607  WRITE(6,2299) (US(IR,IC),IC=1,N)
2299 FORMAT(1X,8F10.5)
601  II=N*ND
     DO 9901 I=1,II
     DO 9901 J=1,II
     IF(I-J)9902,9903,9902
9903 UZ(I,I)=1.0
     US(I,I)=1.0
```

```
      GO TO 9901
 9902 UZ(I,J)=0.0
      UZ(J,I)=0.0
      US(I,J)=0.0
      US(J,I)=0.0
 9901 CONTINUE
      IF(NIX)9002,9002,9003
 9002 WRITE(6,947) TITLE
      IF(II-16)9406,9406,9409
 9406 DO 9407 I=1,II
 9407 WRITE(6,9408) (HZ(I,J),J=1,II)
 9408 FORMAT(2X,16F8.4)
      GO TO 9410
 9409 DO 9419 I=1,II
      WRITE(6,9418) I
 9418 FORMAT(2X,' ROW(',I2,' )')
 9419 WRITE(6,9408) (HZ(I,J),J=1,II)
 9410 DO 9004 M=1,II
 9004 ZR(M)=HZ(M,M)
      IM=II-1
      DO 9005 I=1,IM
      IN=I+1
      DO 9005 J=IN,II
      IF(ABS(ZR(I)-ZR(J))-0.001) 9006,9005,9005
 9006 HIJ=HZ(I,J)
      HII=HZ(I,I)
      HJJ=HZ(J,J)
      HD=ABS(HII-HJJ)
      IF(HD-0.001)9013,9013,9012
 9013 HOG=2.0
      GO TO 9014
 9012 HOG=SIGN(2.0,(HII-HJJ))
 9014 TG=HOG*HIJ/(HD+SQRT(HD*HD+4.*HIJ*HIJ))
      CO=1.0/SQRT(1.+TG*TG)
      SN=TG*CO
      HZ(I,I)=CO*CO*(HII+TG*(2.*HIJ+TG*HJJ))
```

```
      HZ(J,J)=CO*CO*(HJJ-TG*(2.*HIJ-TG*HII))
      HZ(I,J)=0.0
      HZ(J,I)=0.0
      DO 9205 K=1,II
      FF=UZ(K,I)
      UZ(K,I)=CO*FF+SN*UZ(K,J)
      UZ(K,J)=-SN*FF+CO*UZ(K,J)
      IF( (I-K)*(J-K) )9021,9205,9021
 9021 AI=HZ(I,K)
      AJ=HZ(J,K)
      HZ(I,K)=AI*CO+AJ*SN
      HZ(J,K)=-SN*AI+CO*AJ
      AI=HZ(K,I)
      AJ=HZ(K,J)
      HZ(K,J)=-SN*AI+CO*AJ
      HZ(K,I)=AI*CO+AJ*SN
 9205 CONTINUE
 9005 CONTINUE
      IF(NIX)9001,9003,9003
 9003 WRITE(6,948) TITLE
      IF(II-16)9606,9606,9609
 9606 DO 9607 I=1,II
 9607 WRITE(6,9408)(HS(I,J),J=1,II)
      GO TO 9610
 9609 DO 9619 I=1,II
      WRITE(6,9418) I
 9619 WRITE(6,9408)(HS(I,J),J=1,II)
 9610 DO 9104 M=1,II
 9104 ZR(M)=HS(M,M)
      IM=II-1
      DO 9105 I=1,IM
      IN=I+1
      DO 9105 J=IN,II
      IF( ABS(ZR(I)-ZR(J))-.001)9106,9105,9105
 9106 HIJ=HS(I,J)
      HII=HS(I,I)
```

```
      HJJ=HS(J,J)
      HD=ABS(HII-HJJ)
      IF(HD-.001)9113,9113,9112
 9113 HOG=2.0
      GO TO 9114
 9112 HOG=SIGN(2.0,(HII-HJJ))
 9114 TG=HOG*HIJ/(HD+SQRT(HD*HD+4.*HIJ*HIJ))
      CO=1.0/SQRT(1.+TG*TG)
      SN=TG*CO
      HS(I,I)=CO*CO*(HII+TG*(2.*HIJ+TG*HJJ))
      HS(J,J)=CO*CO*(HJJ-TG*(2.*HIJ-TG*HII))
      HS(I,J)=0.0
      HS(J,I)=0.0
      DO 9305 K=1,II
      FF=US(K,I)
      US(K,I)=CO*FF+SN*US(K,J)
      US(K,J)=-SN*FF+CO*US(K,J)
      IF( (I-K)*(J-K) )9121,9305,9121
 9121 AI=HS(I,K)
      AJ=HS(J,K)
      HS(J,K)=-SN*AI+CO*AJ
      HS(I,K)=AI*CO+AJ*SN
      AJ=HS(K,J)
      AI=HS(K,I)
      HS(K,J)=-SN*AI+CO*AJ
      HS(K,I)=AI*CO+AJ*SN
 9305 CONTINUE
 9105 CONTINUE
 9001 JJ=0
      J1=0
      DO 7301 I1=1,N
      DO 7301 JR=1,ND
      AX=0.0
      AY=0.0
      AZ=0.0
      BX=0.0
```

```
      BY=0.0
      BZ=0.0
      J1=J1+1
      DO 7304 I5=1,II
      S1=US(I5,J1)
      Z1=UZ(I5,J1)
      AX=AX+Z1*XD(I5)
      AY=AY+Z1*YD(I5)
      AZ=AZ+Z1*ZD(I5)
      BX=BX+S1*XD(I5)
      BY=BY+S1*YD(I5)
7304  BZ=BZ+S1*ZD(I5)
      XPZ(J1)=AX
      YPZ(J1)=AY
      ZPZ(J1)=AZ
      XPS(J1)=BX
      YPS(J1)=BY
      ZPS(J1)=BZ
      AX1=AX*AX+AY*AY+AZ*AZ
      BX1=BX*BX+BY*BY+BZ*BZ
      AX2=SQRT(AX1)
      BX2=SQRT(BX1)
      AX3=(AX*DLX+AY*DLY+AZ*DLZ)/AX2
      BX3=(BX*DLX+BY*DLY+BZ*DLZ)/BX2
      AX4=(1.-AX3*AX3)
      BX4=(1.-BX3*BX3)
      Z2=(AX*D1X+AY*D1Y+AZ*D1Z)/SQRT(AX1*AX4)
      S2=(BX*D1X+BY*D1Y+BZ*D1Z)/SQRT(BX1*BX4)
      IF(ABS(Z2)-1.0)5661,5661,5662
5662  Z2=SIGN(1.0,Z2)
5661  IF(ABS(S2)-1.0)5663,5663,5664
5664  S2=SIGN(1.0,S2)
5663  CONTINUE
      V(4,I1,JR)=ARCOS(Z2)*57.29578
      V(8,I1,JR)=ARCOS(S2)*57.29578
      AX3=AX4*QN*AX1
```

```
      BX3=BX4*QN*BX1
      VZUM(7,I1,JR)=HZ(J1,J1)
      VZUM(8,I1,JR)=HZ(J1,J1)*AX3
      VSUM(7,I1,JR)=HS(J1,J1)
7301  VSUM(8,I1,JR)=HS(J1,J1)*BX3
      DO 8512 IA=1,N
      DO 8521 J=1,ND
      DO 8522 L5=1,6
      VZUM(L5,IA,J)=0.0
8522  VSUM(L5,IA,J)=0.0
      JJ=JJ+1
      FSX=XPS(JJ)
      FSY=YPS(JJ)
      FSZ=ZPS(JJ)
      FZX=XPZ(JJ)
      FZY=YPZ(JJ)
      FZZ=ZPZ(JJ)
      S1=1.0
      S2=1.0
      Z1=1.0
      Z2=1.0
      GSX=FSX
      GSY=FSY
      GSZ=FSZ
      GZX=FZX
      GZY=FZY
      GZZ=FZZ
      DUMN=DDDZ(JJ)
      DO 8524 K=1,II
      IF(JJ-K)8526,8527,8526
8527  SHD=HS(JJ,JJ)-DUMN
      ZHD=HZ(JJ,JJ)-DUMN
      VSUM(1,IA,J)=VSUM(1,IA,J)+SHD
      VSUM(3,IA,J)=VSUM(3,IA,J)+SHD
      VZUM(3,IA,J)=VZUM(3,IA,J)+ZHD
      VZUM(1,IA,J)=VZUM(1,IA,J)+ZHD
```

```
      GO TO 8524
8526  VZ=HZ(JJ,JJ)-HZ(K,K)
      VS=HS(JJ,JJ)-HS(K,K)
      WZ=HZ(JJ,K)
      WS=HS(JJ,K)
      BS=DDDZ(JJ)-DDDZ(K)
      AX=XPZ(K)
      AY=YPZ(K)
      AZ=ZPZ(K)
      BX=XPS(K)
      BY=YPS(K)
      BZ=ZPS(K)
      IF(ABS(VZ)-.1) 8530,8531,8531
8530  WRITE(6,8532)JJ,K,VZ,VS,BS
8532  FORMAT(1X,'DEGENERACY(',I2,',',I2,')=',F13.8,'VZ',10X,
     1F13.8,'VS',13X,F10.8,'BS')
      GO TO 8535
8531  Z2=Z2+WZ*WZ/(VZ*VZ)
      VZUM(3,IA,J)=VZUM(3,IA,J)+WZ*WZ/VZ
      FZX=FZX+AX*WZ/VZ
      FZY=FZY+AY*WZ/VZ
      FZZ=FZZ+AZ*WZ/VZ
8535  IF(ABS(BS)-.1)8540,8541,8541
8540  WRITE(6,8532)JJ,K,VZ,VS,BS
      GO TO 8544
8541  VZUM(1,IA,J)=VZUM(1,IA,J)+WZ*WZ/BS
      VSUM(1,IA,J)=VSUM(1,IA,J)+WS*WS/BS
      Z1=Z1+WZ*WZ/(BS*BS)
      S1=S1+WS*WS/(BS*BS)
      GSX=GSX+BX*WS/BS
      GSY=GSY+BY*WS/BS
      GSZ=GSZ+BZ*WS/BS
      GZX=GZX+AX*WZ/BS
      GZY=GZY+AY*WZ/BS
      GZZ=GZZ+AZ*WZ/BS
8544  IF(ABS(VS)-.1)8536,8537,8537
```

```
8536 WRITE(6,8532)JJ,K,VZ,VS,BS
     GO TO 8524
8537 VSUM(3,IA,J)=VSUM(3,IA,J)+WS*WS/VS
     S2=S2+WS*WS/(VS*VS)
     FSX=FSX+BX*WS/VS
     FSY=FSY+BY*WS/VS
     FSZ=FSZ+BZ*WS/VS
8524 CONTINUE
     S1=SQRT(S1)
     S2=SQRT(S2)
     Z1=SQRT(Z1)
     Z2=SQRT(Z2)
     VSUM(1,IA,J)=VSUM(1,IA,J)/S1+DUMN
     VZUM(3,IA,J)=VZUM(3,IA,J)/Z2+DUMN
     VZUM(1,IA,J)=VZUM(1,IA,J)/Z1+DUMN
     VSUM(3,IA,J)=VSUM(3,IA,J)/S2+DUMN
     AX=FSX*FSX+FSY*FSY+FSZ*FSZ
     AY=SQRT(AX)
     AZ=(FSX*DLX+FSY*DLY+FSZ*DLZ)/AY
     AY=(1.0-AZ*AZ)
     T22=(FSX*D1X+FSY*D1Y+FSZ*D1Z)/SQRT(AX*AY)
     IF(ABS(T22)-0.999)5671,5671,5672
5672 T22=SIGN(0.99996,T22)
5671 CONTINUE
     V(6,IA,J)=ARCOS(T22)*57.29578
     VSUM(4,IA,J)=AY*QN*AX*VSUM(3,IA,J)/(S2*S2)
     AX=FZX*FZX+FZY*FZY+FZZ*FZZ
     AY=SQRT(AX)
     AZ=(FZX*DLX+FZY*DLY+FZZ*DLZ)/AY
     AY=(1.0-AZ*AZ)
     T22=(FZX*D1X+FZY*D1Y+FZZ*D1Z)/SQRT(AX*AY)
     IF(ABS(T22)-0.999)5677,5677,5678
5678 T22=SIGN(0.99996,T22)
5677 CONTINUE
     V(2,IA,J)=ARCOS(T22)*57.29578
     VZUM(4,IA,J)=AY*QN*AX*VZUM(3,IA,J)/(Z2*Z2)
```

```
      AX=GSX*GSX+GSY*GSY+GSZ*GSZ
      AY=SQRT(AX)
      AZ=(GSX*DLX+GSY*DLY+GSZ*DLZ)/AY
      AY=(1.0-AZ*AZ)
      T22=(GSX*D1X+GSY*D1Y+GSZ*D1Z)/SQRT(AX*AY)
      IF(ABS(T22)-0.999)5673,5673,5674
 5674 T22=SIGN(0.99996,T22)
 5673 CONTINUE
      V(5,IA,J)=ARCOS(T22)*57.29578
      VSUM(2,IA,J)=AY*QN*AX*VSUM(1,IA,J)/(S1*S1)
      AX=GZX*GZX+GZY*GZY+GZZ*GZZ
      AY=SQRT(AX)
      AZ=(GZX*DLX+GZY*DLY+GZZ*DLZ)/AY
      AY=(1.0-AZ*AZ)
      T22=(GZX*D1X+GZY*D1Y+GZZ*D1Z)/SQRT(AX*AY)
      IF(ABS(T22)-0.999)5675,5675,5676
 5676 T22=SIGN(0.99996,T22)
 5675 CONTINUE
      V(1,IA,J)=ARCOS(T22)*57.29578
 8521 VZUM(2,IA,J)=AY*QN*AX*VZUM(1,IA,J)/(Z1*Z1)
 8512 CONTINUE
      IF(NIX)928,928,929
  928 WRITE(6,947) TITLE
  947 FORMAT(1H1,'  PT CH   MATRIX',10X,20A4)
      CALL DIAGIT(II,HZ,N,UZ)
      I3=0
      DO 520 I1=1,N
      DO 520 I2=1,ND
      I3=I3+1
      V(3,I1,I2)=HZ(3,I3)
      VZUM(5,I1,I2)=HZ(1,I3)
  520 VZUM(6,I1,I2)=HZ(2,I3)
      IF(NIX)927,929,929
  929 WRITE(6,948) TITLE
  948 FORMAT(1H1,10X,' DIPOLE MATRIX',10X,20A4)
      CALL DIAGIT(II,HS,N,US)
```

```
      I3=0
      DO521 I1=1,N
      DO 521 I2=1,ND
      I3=I3+1
      V(7,I1,I2)=HS(3,I3)
      VSUM(5,I1,I2)=HS(1,I3)
  521 VSUM(6,I1,I2)=HS(2,I3)
  927 CONTINUE
      READ(5,2120) KOT,(JFA(KO),JFB(KO),KO=1,KOT)
 2120 FORMAT(40I2)
      IF(NIX)2013,2013,2014
 2013 DO 2021 I=1,N
      WRITE(6,2121)TITLE,DLH,DLK,DLL,DLX,DLY,DLZ,D1X,D1Y,D1Z
 2121 FORMAT(1H1,20A4,//,' PT  CH    ENERGIES/OSC STRENGTHS',10X,
     1 ' FACE(',3F3.0,' )'/16X,' NORMAL TO FACE DIR COS    X=',
     2F8.5,5X,' Y=',F8.5,5X,' Z=',F8.5/   1X,' REFERENCE VECTOR FOR ANG
     3CALC DIR COS    X=',F8.5,5X,' Y=',F8.5,5X,' Z=',F8.5/)
      WRITE(6,2125)I
 2125 FORMAT(1X,' FACTOR GROUP FUNCTION NO.',I3,//,
     1'   TRANS',12X,' PERT',14X,' JACOBI',14X,' DIAG',13X,' ORNTD GAS'
     2,13X,' SOLN')
      KK=0
      DO 2021 J=1,NT
      WRITE(6,2123)
      NLEV=INV(J)
 2123 FORMAT(//)
      DO 2021 K=1,NLEV
      KK=KK+1
      WRITE(6,2122)J,K,VZUM(1,I,KK),VZUM(3,I,KK),VZUM(5,I,KK),
     1VZUM(7,I,KK),DDDZ(KK)
 2122 FORMAT(1X,2I3,4X,' E=   ',5(F10.5,10X))
      WRITE(6,2124)VZUM(2,I,KK),VZUM(4,I,KK),VZUM(6,I,KK),VZUM(8,I,KK),
     1ZAD(KK)
 2124 FORMAT(11X,' F=   ',5(F10.5,10X))
      WRITE(6,7124) (V(I1,I,KK),I1=1,4)
 7124 FORMAT(9X,' ANG=   ',4(F10.5,10X),//)
```

```
2021 CONTINUE
     IF(KOT)2032,2032,2031
2031 DO 2033 I=1,KOT
     J=JFA(I)
     K=JFB(I)
     WRITE(6,7103) TITLE,DLH,DLK,DLL
7103 FORMAT(1H1,20A4,//, '   PT  CH     FACE(',3F3.0,' )' )
     WRITE(6,2080) J,K,K,J
2080 FORMAT(///,10X,' SPLITTINGS  E=E(',I2,' )-E(',I2,' )'/10X,
    3' POLARIZATION RATIOS  F(',I2,' )/(',I2,' )'/
    1'   TRANS',12X,' PERT',14X,' JACOBI',14X,' DIAG',13X,' ORNTD GAS'
    2,13X,' SCLN')
     KK=0
     DO 2085 L=1,NT
     WRITE(6,2123)
     NLEV=INV(L)
     DO 2085 M=1,NLEV
     KK=KK+1
     AX=VZUM(2,K,KK)/VZUM(2,J,KK)
     AY=VZUM(4,K,KK)/VZUM(4,J,KK)
     AZ=VZUM(6,K,KK)/VZUM(6,J,KK)
     BX=VZUM(8,K,KK)/VZUM(8,J,KK)
     S1=VZUM(1,J,KK)-VZUM(1,K,KK)
     S2=VZUM(3,J,KK)-VZUM(3,K,KK)
     Z1=VZUM(5,J,KK)-VZUM(5,K,KK)
     Z2=VZUM(7,J,KK)-VZUM(7,K,KK)
     BY =V(1,J,KK)-V(1,K,KK)
     BZ =V(2,J,KK)-V(2,K,KK)
     FSX=V(3,J,KK)-V(3,K,KK)
     FSY=V(4,J,KK)-V(4,K,KK)
     WRITE(6,2122) L,M,S1,S2,Z1,Z2,DDDZ(KK)
     WRITE(6,2124) AX,AY,AZ,BX,ZAD(KK)
2085 WRITE(6,7124)BY,BZ,FSX,FSY
2033 CONTINUE
2032 IF(NIX)8888,2014,2014
2014 DO 2041 I=1,N
```

```
      WRITE(6,2141)TITLE,DLH,DLK,DLL,DLX,DLY,DLZ,D1X,D1Y,D1Z
2141  FORMAT(1H1,20A4,//,' DIPOLE  ENERGIES/OSC STRENGTHS',10X,
     1 ' FACE(',3F3.0,' )'/16X,' NORMAL TO FACE DIR COS    X=',
     2F8.5,5X,' Y=',F8.5,5X,' Z=',F8.5/   1X,' REFERENCE VECTOR FOR ANG
     3CALC DIR COS    X=',F8.5,5X,' Y=',F8.5,5X,' Z=',F8.5/)
      WRITE(6,2125)I
      KK=0
      DO 2041 J=1,NT
      WRITE(6,2123)
      NLEV=INV(J)
      DO 2041 K=1,NLEV
      KK=KK+1
      WRITE(6,2122)J,K,VSUM(1,I,KK),VSUM(3,I,KK),VSUM(5,I,KK),
     1VSUM(7,I,KK),DDDZ(KK)
      WRITE(6,2124)VSUM(2,I,KK),VSUM(4,I,KK),VSUM(6,I,KK),VSUM(8,I,KK),
     1ZAD(KK)
      WRITE(6,7124) (V(I1,I,KK),I1=5,8)
2041  CONTINUE
      IF(KOT)8888,8888,2071
2071  DO 2073 I=1,KOT
      J=JFA(I)
      K=JFB(I)
      WRITE(6,7104) TITLE,DLH,DLK,DLL
7104  FORMAT(1H1,20A4,//,' DIPOLE    FACE(',3F3.0,' )' )
      WRITE(6,2080) J,K,K,J
      KK=0
      DO 2095 L=1,NT
      WRITE(6,2123)
      NLEV=INV(L)
      DO 2095 M=1,NLEV
      KK=KK+1
      AX=VSUM(2,K,KK)/VSUM(2,J,KK)
      AY=VSUM(4,K,KK)/VSUM(4,J,KK)
      AZ=VSUM(6,K,KK)/VSUM(6,J,KK)
      BX=VSUM(8,K,KK)/VSUM(8,J,KK)
      S1=VSUM(1,J,KK)-VSUM(1,K,KK)
```

```
      S2=VSUM(3,J,KK)-VSUM(3,K,KK)
      Z1=VSUM(5,J,KK)-VSUM(5,K,KK)
      Z2=VSUM(7,J,KK)-VSUM(7,K,KK)
      WRITE(6,2122) L,M,S1,S2,Z1,Z2,DDDZ(KK)
      BY =V(5,J,KK)-V(5,K,KK)
      BZ =V(6,J,KK)-V(6,K,KK)
      FSX=V(7,J,KK)-V(7,K,KK)
      FSY=V(8,J,KK)-V(8,K,KK)
      WRITE(6,2124) AX,AY,AZ,BX,ZAD(KK)
2095  WRITE(6,7124)BY,BZ,FSX,FSY
2073  CONTINUE
8888  CONTINUE
      MG=MG-1
      GO TO 7000
 328  STOP
      END
      SUBROUTINE DIAGIT(N,H,KN,U)
      DIMENSION XD(32),YD(32),ZD(32),X(32),IQ(32),H(32,32),U(32,32)
      COMMON XD,YD,ZD,DLX,DLY,DLZ,D1X,D1Y,D1Z
1035  WRITE (6,5)
    5 FORMAT(//,20X,' INPUT MATRIX')
      IF(N-16)6,6,9
    6 DO 7 I=1,N
    7 WRITE (6,8)(H(I,J),J=1,N)
    8 FORMAT(2X,16F7.3)
      GO TO 21
    9 DO 19 I=1,N
      WRITE (6,18)I
   18 FORMAT(2X,' ROW(',I2,' )')
   19 WRITE (6,8)(H(I,J),J=1,N)
   21 RAP=7.45E-9
      HDTEST=1.0E38
      IF(N-2)9001,9002,15
9002  HIJ=H(1,2)
      HII=H(1,1)
      HJJ=H(2,2)
```

```
      HD=ABS(HII-HJJ)
      HDG=SIGN(2.0,(HII-HJJ))
      TG=HDG*HIJ/(HD+SQRT(HD*HD+4.*HIJ*HIJ))
      CO=1.0/SQRT(1.+TG*TG)
      SN=TG*CO
      H(1,1)=CO*CO*(HII+TG*(2.*HIJ+TG*HJJ))
      H(2,2)=CO*CO*(HJJ-TG*(2.*HIJ-TG*HII))
      U(1,1)=CO
      U(1,2)=-SN
      U(2,1)=SN
      U(2,2)=CO
      GO TO 9001
   15 NR=0
   17 NMI1=N-1
      DO 30 I=1,NMI1
      X(I)=0.
      IPL1=I+1
      DO 30 J=IPL1,N
      IF (X(I)-ABS(H(I,J)))20,20,30
   20 X(I)=ABS(H(I,J))
      IQ(I)=J
   30 CONTINUE
   40 IPIV=1
      JPIV=IQ(1)
      XMAX=X(1)
      DO 70 I=2,NMI1
      IF (XMAX-X(I))60,70,70
   60 XMAX=X(I)
      IPIV=I
      JPIV=IQ(I)
   70 CONTINUE
      IF (XMAX)1000,1000,80
   80 IF (HDTEST)90,90,85
   85 IF (XMAX-HDTEST)90,90,148
   90 HDIMIN=ABS(H(1,1))
      DO 110 I=2,N
```

```
      IF (HDIMIN-ABS(H(I,I)))110,110,100
  100 HDIMIN=ABS(H(I,I))
  110 CONTINUE
      HDTEST=HDIMIN*RAP
      IF (HDTEST-XMAX)148,1000,1000
  148 NR=NR+1
  150 TANG=SIGN(2.0,(H(IPIV,IPIV)-H(JPIV,JPIV)))*H(IPIV,JPIV)/(ABS(H(
     1IPIV,IPIV)-H(JPIV,JPIV))+SQRT((H(IPIV,IPIV)-H(JPIV,JPIV))**2+4.0*H
     1(IPIV,JPIV)**2))
      COSINE=1.0/SQRT(1.0+TANG**2)
      SINE=TANG*COSINE
      HII=H(IPIV,IPIV)
      H(IPIV,IPIV)=COSINE**2*(HII+TANG*(2.*H(IPIV,JPIV)+TANG*H(JPIV,JPIV
     1)))
      H(JPIV,JPIV)=COSINE**2*(H(JPIV,JPIV)-TANG*(2.*H(IPIV,JPIV)-TANG*
     1HII))
      H(IPIV,JPIV)=0.
      DO 350 I=1,NMI1
      IF (I-IPIV)210,350,200
  200 IF (I-JPIV)210,350,210
  210 IF (IQ(I)-IPIV)230,240,230
  230 IF (IQ(I)-JPIV)350,240,350
  240 K=IQ(I)
  250 HTEMP=H(I,K)
      H(I,K)=0.
      IPL1=I+1
      X(I)=0.
      DO 320 J=IPL1,N
      IF (X(I)-ABS(H(I,J)))300,300,320
  300 X(I)=ABS(H(I,J))
      IQ(I)=J
  320 CONTINUE
      H(I,K)=HTEMP
  350 CONTINUE
      X(IPIV)=0.
      X(JPIV)=0.
```

```
      DO 530 I=1,N
      IF (I-IPIV)370,530,420
  370 HTEMP=H(I,IPIV)
      H(I,IPIV)=COSINE*HTEMP+SINE*H(I,JPIV)
      IF (X(I)-ABS(H(I,IPIV)))380,390,390
  380 X(I)=ABS(H(I,IPIV))
      IQ(I)=IPIV
  390 H(I,JPIV)=-SINE*HTEMP+COSINE*H(I,JPIV)
      IF (X(I)-ABS(H(I,JPIV)))400,530,530
  400 X(I)=ABS(H(I,JPIV))
      IQ(I)=JPIV
      GO TO 530
  420 IF (I-JPIV)430,530,480
  430 HTEMP=H(IPIV,I)
      H(IPIV,I)=COSINE*HTEMP+SINE*H(I,JPIV)
      IF (X(IPIV)-ABS(H(IPIV,I)))440,450,450
  440 X(IPIV)=ABS(H(IPIV,I))
      IQ(IPIV)=I
  450 H(I,JPIV)=-SINE*HTEMP+COSINE*H(I,JPIV)
      IF (X(I)-ABS(H(I,JPIV)))400,530,530
  480 HTEMP=H(IPIV,I)
      H(IPIV,I)=COSINE*HTEMP+SINE*H(JPIV,I)
      IF (X(IPIV)-ABS(H(IPIV,I)))490,500,500
  490 X(IPIV)=ABS(H(IPIV,I))
      IQ(IPIV)=I
  500 H(JPIV,I)=-SINE*HTEMP+COSINE*H(JPIV,I)
      IF (X(JPIV)-ABS(H(JPIV,I)))510,530,530
  510 X(JPIV)=ABS(H(JPIV,I))
      IQ(JPIV)=I
  530 CONTINUE
      DO 550 I=1,N
      HTEMP=U(I,IPIV)
      U(I,IPIV)=COSINE*HTEMP+SINE*U(I,JPIV)
  550 U(I,JPIV)=-SINE*HTEMP+COSINE*U(I,JPIV)
      GO TO 40
 1000 CONTINUE
```

```
9001 DO 600 I=1,N
 600 WRITE (6,610)I,H(I,I)
 610 FORMAT(10X,' E(',I2,' )=',F12.5)
     WRITE (6,620)
 620 FORMAT(//,10X,' EIGENVECTORS')
     IF(N-16)625,625,700
 700 DO 770 I=1,N
     WRITE (6,710)I
 710 FORMAT(2X,' ROW(',I2,' )')
 770 WRITE (6,640)(U(J,I),J=1,N)
     GO TO 645
 625 DO 630 I=1,N
 630 WRITE (6,640)(U(J,I),J=1,N)
 640 FORMAT(2X,16F7.3)
 645 WRITE (6,650)NR
 650 FORMAT (////,58X,4H NR=,I5)
     DO 711 K=1,N
 711 H(1,K)=H(K,K)
     DO 721 M=1,N
     A=0.0
     B=0.0
     C=0.0
     DO 722 K=1,N
     UG=U(K,M)
     A=A+UG*XD(K)
     B=B+UG*YD(K)
 722 C=C+UG*ZD(K)
     G=A*A+B*B+C*C
     F=SQRT(G)
     AW=(A*DLX+B*DLY+C*DLZ)/F
     BW=1.-AW*AW
     T22=(A*D1X+B*D1Y+C*D1Z)/SQRT(G*BW)
     IF(ABS(T22)-0.99996)5661,5661,5662
5662 T22=SIGN(0.99996,T22)
5661 CONTINUE
     H(3,M)=ARCOS(T22)*57.29578
```

```
721  H(2,M)=BW*G*H(1,M)*0.0004703/KN
     RETURN
     END
```

BIBLIOGRAPHY

1. J. Frenkel, Phys. Rev., 37, 17 (1931).

2. D. P. Craig and T. Thirunamachandran, Proc. Phys. Soc. (London), 84, 781 (1964).

3. R. Silbey, J. Jortner, and S. A. Rice, J. Chem. Phys., 42, 1515 (1965).

4. H. C. Longuet-Higgins, Proc. Roy. Soc., A235, 537 (1956).

5. S. C. Neely, Ph.D. Dissertation, Yale University, 1965.

6. J. J. Hopfield, Phys. Rev., 112, 1555 (1958).

7. R. M. Hochstrasser, Ann. Rev. Phys. Chem., 17, 457 (1966).

8. D. P. Craig and S. H. Walmsley, Physics and Chemistry of the Organic Solid State, 1, 586 (1963).

9. R. Silbey and S. A. Rice, Physics and Chemistry of the Organic Solid State, 3, 204 (1965).

10. D. P. Craig, S. A. Walmsley, Excitons in Molecular Crystals, (W. A. Benjamin, Inc., New York), 1968.

11. A. S. Davydov, Theory of Molecular Excitons, (Plenum Press, Inc., New York), 1972.

12. V. M. Agranovitch, Zh. Eks. Teor. Fiz., 37, 430 (1959). Sov. Phys. - JETP 10, 307 (1960).

13. V. Fano, Phys. Rev., 103, 1202 (1956); 118, 451 (1960).

14. L. B. Clark and M. R. Philpott, J. Chem. Phys., 53, 3790 (1970).

15. L. E. Lyons and G. C. Morris, J. Chem. Soc., 159, 2766 (1956).

16. W. T. Simpson and D. L. Peterson, J. Chem. Phys., 26, 588 (1957).

17. R. M. Hochstrasser, Molecular Aspects of Symmetry, (W. A. Benjamin, Inc., New York), 1966.

18. H. Winston and R. S. Halford, J. Chem. Phys., 17, 607 (1949).

19. P. P. Ewald, Annls Phys., 49, 1 (1916).

20. M. Born and K. Huang, Dynamical Theory of Crystal Lattices, (Oxford University Press, London), 1954.

21. R. W. Ditchburn, Light, 2nd Ed., (Interscience Publishers, New York), 1963.

22. W. Heitler, The Quantum Theory of Radiation, 3rd Ed., (Clarendon Press, Oxford), 1954.

23. D. W. J. Cruickshank, Acta. Cryst., 9, 915 (1956).

24. J. M. Robertson, V. C. Sinclair and J. Trotter, Acta. Cryst., 14, 697 (1961).

25. M. R. Philpott, J. Chem. Phys., 58, 588 (1973).

26. M. A. Ball and A. D. McLachlan, Proc. Roy. Soc., A282, 433 (1964).

27. M. R. Philpott, J. Chem. Phys., 50, 3925 (1969).

28. M. R. Philpott, J. Chem. Phys., 54 2120 (1971).

29. D. P. Craig and L. A. Dissado, Proc. Roy. Soc., A325, 1 (1971).

30. M. Tanaka and J. Tanaka, Molec. Phys., 16, 1 (1969).

31. M. R. Philpott, J. Chem. Phys., 50 , 5117 (1969).

32. L. B. Clark, J. Chem. Phys., 53, 4092 (1970).

33. L. B. Clark, J. Chem. Phys., 51, 5719 (1969).

34. A. R. Lacey and L. E. Lyons, Proc. Chem. Soc., 414 (1960).

35. T. A. Claxton, D. P. Craig, and Thirunamachandran, J. Chem. Phys., 35, 1525 (1961).

36. A. Bree and L. E. Lyons, Proc. Chem. Soc. 2662 (1956).

37. A. R. Lacey and L. E. Lyons, Proc. Chem. Soc., 5393 (1964).

38. J. W. Sidman, Phys. Rev., 102, 96 (1956).

39. A. Matsui and Y. Ishii, J. Phys. Soc. Japan, 23, 581 (1967).

40. D. P. Craig, J. Chem. Soc., 158, 2302 (1955).

41. A. Streitwieser, Jr., Molecular Orbital Theory for Organic Chemists, (John Wiley and Sons, Inc., New York), 1962.

42. QCPE program 71.2, Quantum Chemistry Program Exchange, Indiana University, Bloomington, Indiana.

43. A. Bree and L. E. Lyons, J. Chem. Soc., 164, 5206 (1960).

44. G. D. Mahan, J. Chem. Phys., 41, 2930 (1964).

45. A. Mathieson, J. M. Robertson, and V. C. Sinclair, Acta. Cryst., 3, 245 (1950).

46. R. Mason, Acta. Cryst., 17, 547 (1964).

47. J. Tanaka, Bull. Chem. Soc. Japan, 38, 86 (1965).

48. G. C. Morris, J. Mol. Spectry., 18, 42 (1965).

49. D. P. Craig and Thirunamachandran, Bull. Sci. Fac. Chim. Ind. Bologna, 21, 15 (1963).